Pressure-Induced Cycloadditions of Dicyanoacetylene to Strained Arenes: The Formation of Cyclooctatetraene, 9,10-Dihydronaphthalene, and Azulene Derivatives; A Degenerate [1,5] Sigmatropic Shift—Comparison between Theory and Experiment

Frank-Gerrit Klärner,*[a] Ralf Ehrhardt,[a] Heinz Bandmann,[a] Roland Boese,*[b] Dieter Bläser,[b] K. N. Houk,*[c] and Brett R. Beno[c]

Dedicated to Professor Reiner Sustmann on the occasion of his 60th birthday

Abstract: The reaction of dicyanoacetylene (DCA) with the partially hydrogenated dimethano-bridged anthracene and pentacene derivatives **3** and **18** lead to the (1:1) Diels–Alder adducts **5** and **19**, respectively, and to the 9,10-dihydronaphthalene derivatives **6** and **21**, respectively. These compounds are intensely colored, most likely due to a charge-transfer absorption. Photolysis of the (1:1) adducts **5** and **19** produces the corresponding cyclooctatetraene derivatives **7** and **8**, which are not planar despite the torsional constraints caused by the fusion of the eight-membered ring to norbornane and norbornene units. The mechanisms of formation of the dihydronaphthalene derivatives **6** and **21** were elucidated by the use of high pressure; this allowed the (2:1) adducts **11** and **20** to be detected as intermediates in the reaction of DCA with **5** or **19** to give **6** and **21**, respectively. A degenerate rearrangement consisting formally of a [1,5] vinyl shift in **6** or **21** could be detected by their temperature-dependent ^{1}H NMR spectra. The mechanisms of the [1,5]-sigmatropic-shift reactions in **6** and **24** have been examined at the Becke3LYP/6-31G* level of theory. Stepwise mechanisms are predicted, and the calculated activation barrier is in good agreement with the measured $\Delta H^{\neq}$. The finding that the irreversible rearrangement of **6** accompanied by the elimination of HCN to give the azulene derivative **14** proceeds only on heating of **6** to 80 °C in a polar solvent is good evidence for a polar mechanism in this case.

Keywords: ab initio calculations · charge transfer · Diels–Alder cycloadditions · high-pressure chemistry · NMR spectroscopy · sigmatropic rearrangements

Introduction

The planarization of the 1,3,5-cycloheptatriene skeleton, which usually exists in a boat conformation, could be achieved by fixation of one of the torsional angles to 0° by fusion of a rigid norbornane unit at C-1 and C-7 of the cycloheptatriene ring.[1] According to Dreiding molecular model considerations it should be possible to fix 1,3,5,7-cyclooctatetraene (COT) in a planar conformation by fusion of two norbornane units with the carbon atoms C-1, C-2 and C-4, C-5 of the eight-membered ring. The introduction of two torsional constraints is necessary to avoid a rapid π-bond shift to foil planarization of the eight-membered ring.[1, 2] Planar COT derivatives are interesting compounds with respect to the question of their antiaromaticity.[2, 3] Hitherto, only two derivatives are known, which according to crystal structure analyses contain planar eight-membered rings with π bonds tending toward localization.[4] Recently, the parent planar COT has been observed by means of transition-state spectroscopy. Accordingly, the singlet lies well below the triplet D_{8h} COT in agreement with ab initio predictions that COT violates Hund's rule.[3] Here we report the synthesis and the structural properties of a dicyano derivative of **1**. Furthermore, in the reaction of dicyanoace-

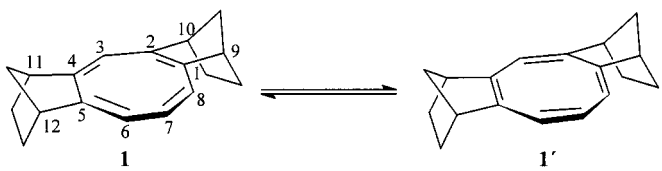

1 **1′**

[a] Prof. Dr. F.-G. Klärner, Dipl.-Chem. R. Ehrhardt, H. Bandmann
Institut für Organische Chemie, Universität GH Essen
D-45117 Essen (Germany)
Fax: (+49) 201-183-3082
E-mail: klaerner@oc1.orgchem.uni-essen.de

[b] Prof. Dr. R. Boese, D. Bläser
Institut für Anorganische Chemie, Universität GH Essen
D-45117 Essen (Germany)

[c] Prof. Dr. K. N. Houk, Dr. B. R. Beno
Department of Chemistry and Biochemistry, University of California
Los Angeles, CA 90095-1569 (USA)

  0947-6539/99/0507-2119 $ 17.50+.50/0

tylene with the strained arene derivatives **3** and **18**, we discovered the formation of the unexpected dark blue 9,10-dihydronaphthalene derivatives **6** and **21**. These undergo degenerate [1,5] sigmatropic shifts that are rapid on the NMR time scale. Ab initio calculations at the Becke3LYP/6-31G* hybrid HF-DFT level suggest a stepwise process for the degenerate [1,5] shift.

Results and Discussion

Synthesis and reactions of 1,2,3,4,5,6,7,8-octahydro-1,4:5,8-dimethanoanthracene (3): Octahydrodimethanoanthracene **3** is prepared by a highly stereoselective Diels–Alder reaction of 2,3-bismethylenenorbornane[5] with norbornene followed by DDQ oxidation of the major adduct *endo,exo*-**2**[6] (DDQ = 2,3-dichloro-5,6-dicyano-1,4-benzoquinone; Scheme 1). The *syn* configuration of the two methano bridges in *endo,exo*-**2** was assigned by crystal structure analysis of the corresponding epoxide **4** (Figure 1) obtained either by repeated recrystallization of *endo,exo*-**2** in air or by air oxidation of *endo,exo*-**2** in CH_2Cl_2 (40 °C, 24 h, yield: 44 %). This is another remarkable example of the epoxidation of a polycyclic strained olefin that simply proceeds by its reaction with molecular oxygen without any catalyst.[7] Conventional epoxidation of *endo,exo*-**2** with *m*-CPBA also produces **4**.

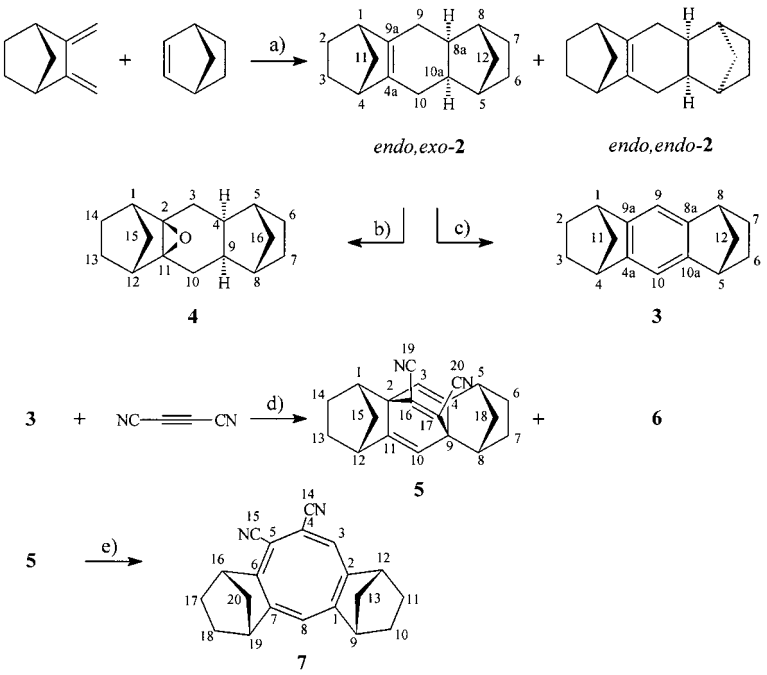

Scheme 1. Formation and reactions of octahydrodimethanoanthracene **3**. a) 1 bar, 160 °C, *endo,exo*-**2** and *endo,endo*-**2** formed in the ratio of 88:12, yield of *endo,exo*-**2** (colorless crystals, m.p. 35 °C) after recrystallization from ethanol: 50 %; 7.9 kbar, 75 °C, 6 h, *endo,exo*-**2** and *endo,endo*-**2** formed in the ratio of 96:4; conversion of the diene: 30 %. b) *m*-Chloroperbenzoic acid, 5 °C, 16 h, CH_2Cl_2, yield: 80 %; O_2, 40 °C, 24 h, CH_2Cl_2, yield: 44 %. c) DDQ, 80 °C, 2 h, toluene, yield: > 99 %. d) 1 bar, 127 °C, 17 h, **3**, **5** and **6** formed in the ratio of 30:56:14 (^{1}H NMR), yield: 49 % of **5** (colorless crystals, m.p. 192 °C) and 11 % of **6** (dark blue crystals, m.p. 159 °C, decomp); 9 kbar, 83 °C, 17 h, **3**, **5** and **6** formed in the ratio of 64:13:23 (^{1}H NMR). e) *hv* (300 nm), 45 min, hexane, acetone (10:1), yield: 68 % of **7** (red-orange crystals, m.p. 151 °C).

Abstract in German: *Die Reaktion von Dicyanacetylen (DCA) mit den partiell hydrierten, dimethanoüberbrückten Anthracen- und Pentacenderivaten* ***3*** *und* ***18*** *liefert die 1:1-Diels-Alder-Addukte* ***5*** *bzw.* ***19*** *sowie die 9,10-Dihydronaphthalinderivate* ***6*** *bzw.* ***21****. Die intensive Blaufärbung von* ***6*** *und* ***21*** *stammt von einer Absorption, die höchstwahrscheinlich einem Charge-Transfer-Übergang zuzuordnen ist. Die Photolyse der 1:1-Addukte* ***5*** *und* ***19*** *führt zu den entsprechenden Cyclooctatetraenderivaten* ***7*** *und* ***18****, die trotz der durch die anellierten Norbornan- und Norborneneinheiten verursachten Torsionsspannung nicht planar sind. Der Mechanismus für die Bildung der Dihydronaphthaline* ***6*** *und* ***21*** *ließ sich mit Hilfe von hohem Druck aufklären. In der zu* ***6*** *bzw.* ***21*** *als Endprodukte führenden Reaktion von DCA mit* ***5*** *oder* ***19*** *bei hohem Druck war es möglich, die 2:1-Addukte* ***11*** *und* ***20*** *als Zwischenprodukte nachzuweisen. Durch temperaturabhängige ^{1}H-NMR-Spektroskopie wurde eine entartete Umlagerung der Systeme* ***6*** *und* ***21*** *beobachtet, die formal als eine sigmatrope [1,5]Vinylverschiebung aufzufassen ist. Nach DFT-Berechnung (Becke3LYP/6-31G*) handelt es sich bei dieser Umlagerung um einen mehrstufigen Prozeß. Die berechnete Aktivierungsbarriere stimmt gut mit dem experimentell bestimmten $\Delta H^{\neq}$-Wert überein. Die Beobachtung, daß die von einer HCN-Eliminierung begleitete, irreversible Umlagerung von* ***6*** *in das Azulenderivat* ***14*** *nur bei der Thermolyse von* ***6*** *in polaren Lösungsmitteln stattfindet, spricht für einen polaren Mechanismus dieser Reaktion.*

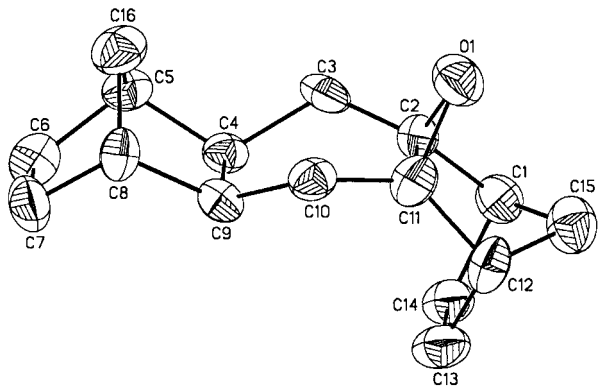

Figure 1. Crystal structure analysis of **4** (50 % ellipsoids)

The reaction of **3** with dicyanoacetylene (DCA) leads to the (1:1) Diels–Alder adduct **5** and to the unexpected dark blue (2:1) adduct **6** (Scheme 1). The course of the reaction can be controlled by the concentration of DCA and, to some extent, by pressure. At atmospheric pressure (ca. 1 bar) the (1:1) adduct **5** is the major product after 70 % conversion of **3**, whereas at high pressure (9 kbar) the (2:1) adduct **6** dominates even after 36 % conversion of **3**. The synthesis of the cyclooctatetraene derivative **7** starting from **5** was feasible in light of the known synthesis of 1,2-dicyanocyclooctatetraene

  0947-6539/99/0507-2120 $ 17.50+.50/0 *Chem. Eur. J.* **1999**, *5*, No. 7

by the photochemically induced rearrangement of 2,3-dicyanobarrelene.[8] The photolysis of **5** (separated from **6** by liquid chromatography) produces the desired COT derivative **7** in 68% yield (Scheme 1).

The crystal structure analysis shows that the eight-membered ring in **7** is not planar, contrary to the predictions,[1] with alternating bond lengths characteristic for conjugated polyenes. Accordingly, the distortion of the fused bismethylenenorbornane unit by 16.7° (dihedral angle ⟨16,6,7,19⟩) is sufficient to avoid a planar COT structure. The structural parameters obtained by the crystal structure analysis of **7** are in reasonable agreement with those obtained by semiempirical PM3 calculations.[9] Table 1 shows a comparison between experimental and calculated bond lengths and dihedral angles. The dihedral angles in the eight-membered ring of **7** that are responsible for its boat conformation are comparable with the corresponding angle of the parent cyclooctatetraene (⟨1,2,3,4⟩ = 56°).[10] From the PM3 calculations, the cyano groups at C-4 and C-5 in **7** should not exhibit a significant effect on the COT structure. Also according to PM3 calculations (Figure 2), the more rigid torsional constraints in **8**, **9**, and **10** lead to a significant but not complete planarization of the COT skeleton. We have tried to test these predictions with the synthesis of **8** and **10**; we succeeded in the case of **8**, but failed in the case of **10**. These experiments will be discussed later.

Table 1. Experimental and calculated (PM3) bond lengths and dihedral angles of **7**.

	bond lengths [Å]			dihedral angles [°]	
	exptl	calcd		exptl	calcd
C1–C2	1.340	1.355	⟨1,2,3,4⟩	54.2	52.4
C2–C3	1.450	1.442	⟨3,4,5,6⟩	59.5	59.6
C3–C4	1.345	1.342	⟨5,6,7,8⟩	47.5	38.6
C4–C5	1.498	1.475	⟨7,8,1,2⟩	43.9	45.0
C5–C6	1.335	1.347	⟨16,6,7,19⟩	16.7	13.5
C6–C7	1.477	1.476	⟨9,1,2,12⟩	0.9	0.2

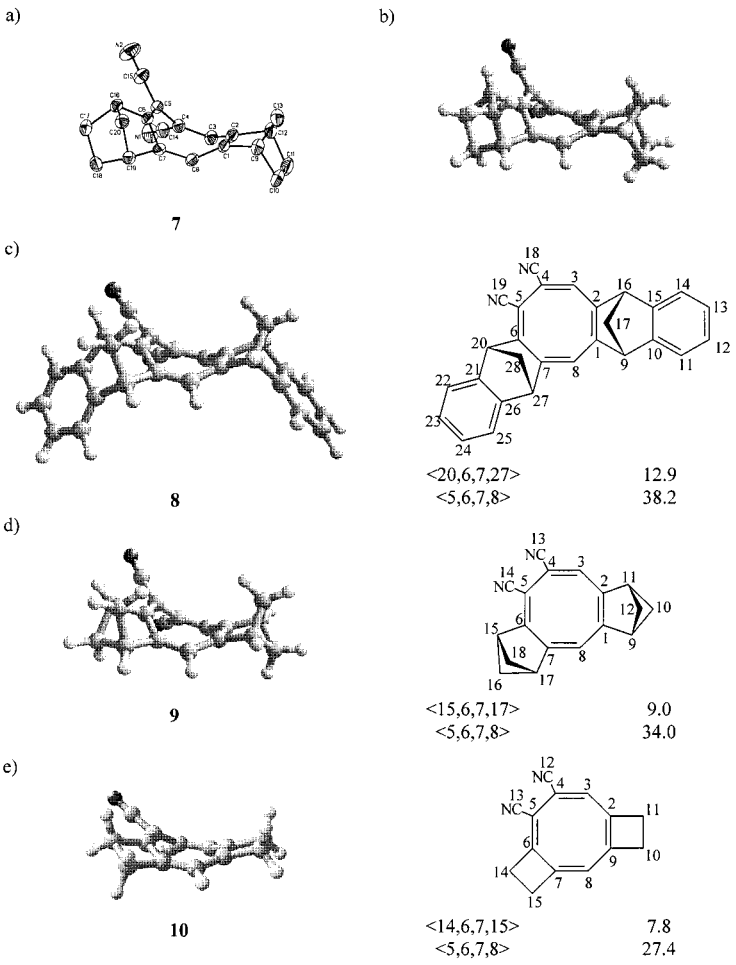

Figure 2. a) Crystal structure of **7** (50% ellipsoids). b), c), d), e) Structures of **7**, **8**, **9**, and **10**, respectively, calculated by PM3.

The structure of the dark blue (2:1) adduct was elucidated by crystal structure analysis and found to be the *cis*-9,10-dihydronaphthalene derivative **6** (Figure 3). The mechanism of formation of **6** could be determined by high-pressure studies. The reaction of **5** with DCA at 1 bar and 127 °C leads to **6** only; this indicates that the (1:1) adduct **5** is an intermediate in the reaction **3** + DCA → **6**. At 12 kbar **5** reacts with DCA readily at room temperature to produce the colorless homo-Diels–Alder adduct **11** (Scheme 2), which undergoes a rearrangement (retro-Diels–Alder reaction) to the blue dihydronaphthalene derivative **6** either at room temperature (half-life of **11** at 20 °C: ca. 28 d) or at 60° C (half-life: 42 min, $\Delta G^{\ddagger} = 24.1$ kcal mol^{-1}).

Compound **6** undergoes a degenerate rearrangement **6** ⇌ **6′**, which is rapid on the NMR time scale at room temperature, leading to a pairwise exchange of the signals assigned to the four chemically nonequivalent norbornene or *exo*-methylenenorbornane bridgehead hydrogen atoms. From the temperature-dependent line shape of these signals the activation parameters can be determined (Figure 3, Table 2).

Analogous but nondegenerate rearrangements have been observed by L. A. Paquette et al.[11] and G. Maier et al.[12] in the thermolyses of other *cis*-9,10-dihydronaphthalene derivatives (*cis*-9,10-dimethyl-9,10-dihydronaphthalene: $\Delta H^{\ddagger} = 25.4 \pm 0.5$ kcal mol^{-1}, $\Delta S^{\ddagger} = -2.1 \pm 1.6$ cal mol^{-1} K^{-1}, 61.3 °C; *cis*-9,10-dicarbomethoxy-9,10-dihydronaphthalene: $\Delta H^{\ddagger} = 25.7 \pm 0.4$ kcal mol^{-1}, $\Delta S^{\ddagger} = -6.3 \pm 1.2$ cal mol^{-1} K^{-1}, 81.2 °C, and 1,2,3,4,5,6,7,8-octamethyl-*cis*-9,10-dimethoxymethyl-9,10-dihydro-naphthalene: $\Delta G^{\ddagger} \approx 25$ kcal mol^{-1}, 20 °C). The enthalpies of activation of these rearrangements are substantially higher than those found for the degenerate rearrangement in **6** (Table 2). This difference may be the result of the steric effect of the fused norbornene units on the 9,10-dihydronaphthalene system and of the electronic effect of the four cyano groups on the potential intermediate of this rearrangement (vide infra). In the polar solvent CD_3OD a higher enthalpy of activation is found for the rearrangement of **6** than in the less polar solvents CD_2Cl_2 and [D_8]toluene; this is compensated by its larger entropy of activation, so that the Gibbs enthalpy of activation in CD_3OD is comparable with that determined in CD_2Cl_2 or [D_8]toluene. Since precise measurement of absolute temperatures in the NMR spectrometer is difficult, $\Delta H^{\ddagger}$ and $\Delta S^{\ddagger}$ determined from the temperature dependence of the NMR signals frequently have large errors in contrast to the $\Delta G^{\ddagger}$ values, which are

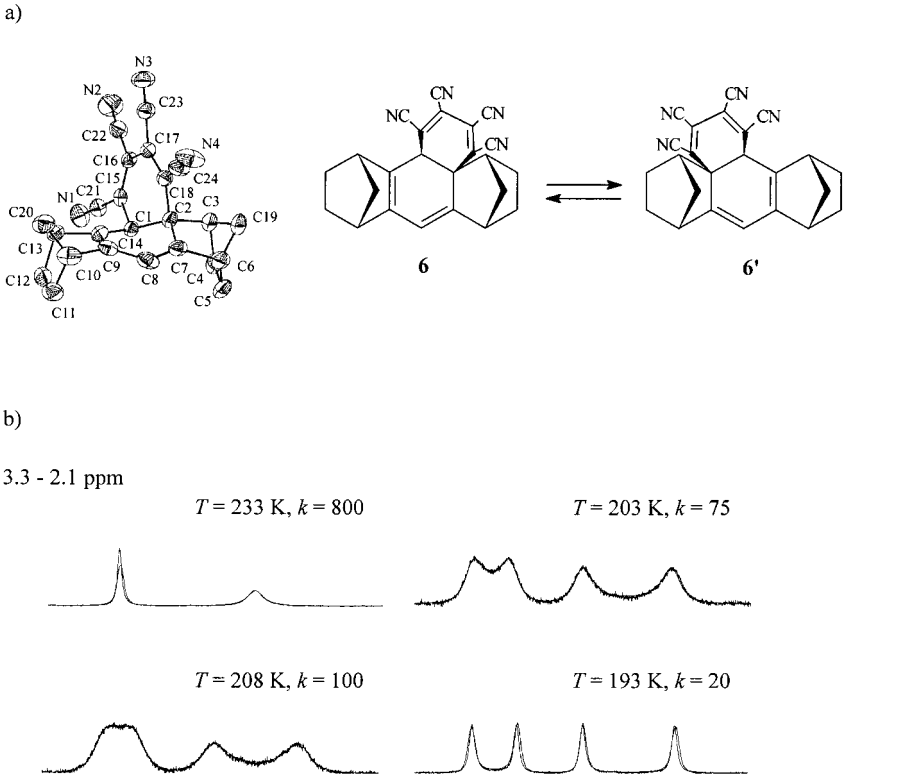

Figure 3. a) Crystal structure analysis of **6** (50% ellipsoids). b) Temperature-dependent ^{1}H NMR (300 MHz, CD_2Cl_2) of the bridgehead hydrogen atoms 3-H, 13-H at $\delta = 2.60$ and 6-H, 10-H at $\delta = 3.08$; the experimental spectra and the spectra calculated by line-shape analysis with the rate constants k [s^{-1}] of the mutual exchange at various temperatures T [K] are superimposed.

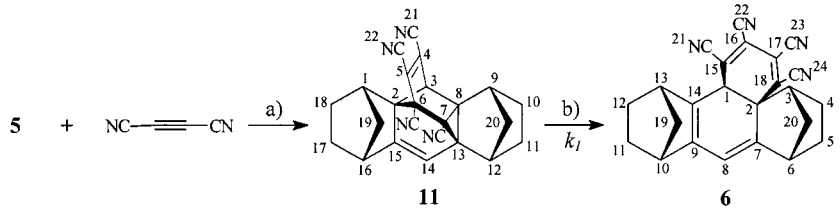

Scheme 2. Reaction scheme of the formation of **6**. a) 1 bar, 127 °C, 17 h, **5** and **6** formed in the ratio of 42:58 (^{1}H NMR), yield 45% of **6**; 12 kbar, 20 °C, 90 h, **5**, **11** and **6** formed in the ratio of 49:40:11, yield: 35% of **11** (colorless crystals), 9% of **6**. b) 1 bar, 60.0 °C, 110 min, conversion: 84.8%, $k_1 = (2.74 \pm 0.19) \times 10^{-4}\ s^{-1}$, $\Delta G^{\neq} = 24.1$ kcal mol^{-1}).

Table 2. Activation parameters $\Delta H^{\neq}$ and $\Delta G^{\neq}$ in kcal mol^{-1} and $\Delta S^{\neq}$ in cal mol^{-1} K^{-1} of the degenerate rearrangement in **6** obtained by temperature-dependent ^{1}H NMR spectroscopy in different solvents.

	$\Delta H^{\neq}$	$\Delta S^{\neq}$	$\Delta G^{\neq}$
CD_2Cl_2	7.7 ± 0.5	-12 ± 2	10.2 ± 0.7
[D_8]Toluene	7.3 ± 0.5	-14 ± 2	10.3 ± 0.6
CD_3OD	12.0 ± 0.4	4 ± 2	11.1 ± 0.6

determined at one temperature only, mostly at the temperature of coalescence.[13] In the case of **6**, however, the kinetic measurements rely on the coalescence of two pairs of signals occurring at different temperatures owing to the different $\Delta\tilde{\nu}$ values of the exchanging signals (3-H $\Leftrightarrow$ 13-H: $\Delta\tilde{\nu} = 100$ Hz, 6-H $\Leftrightarrow$ 10-H: $\Delta\tilde{\nu} = 50$ Hz). Furthermore, the solvent dependence of activation parameters were determined in the same temperature range with the same NMR spectrometer, so that the differences in the activation parameter seem to be significant here. Entropy–enthalpy compensation in solvation is frequently observed and agrees with the intuition that a stronger enthalpic interaction between molecules results in a reduction of the configurational freedom of the system and, thus, in a reduction of entropy. Corrrespondingly, weaker intermolecular enthalpic interactions produce a looser molecular association and an increase in entropy.[14] In the case of the degenerate rearrangement of **6**, the observation that enthalpy and entropy of activation are larger in CD_3OD than in CD_2Cl_2 or [D_8]toluene indicates that the ground state is more polar than the transition state.

On thermolysis at 80 °C in a polar solvent such as acetonitrile (half-life: 110 min) or methanol (half-life: 120 min), **6** undergoes an irreversible rearrangement accompanied by an HCN elimination to give the azulene derivative **14**[15] in quantitative yield (Figure 4). However, in the less polar solvent toluene **6** is stable up to 150 °C. In order to explain this remarkable reaction we suggest a reversible disrotatory electrocyclic ring-opening of **6** to give the all-*cis*-cyclodecapentaene **12** followed by a disrotatory orbital symmetry-allowed electrocyclization to form the dipolar intermediate **13** in the rate-determining step (Scheme 3); this explains the solvent dependence of the overall reaction. Finally HCN is eliminated from **13**, probably in a stepwise process, to produce the observed azulene **14**.

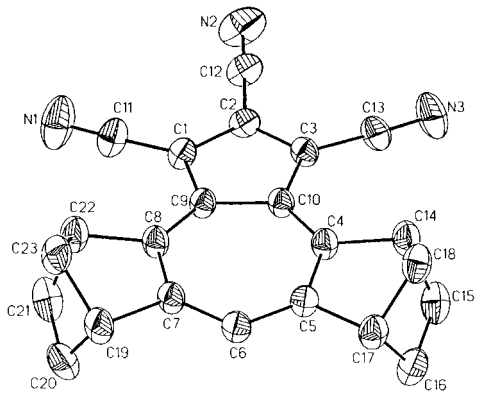

Figure 4. Crystal structure analysis of **14** (50% ellipsoids)

0947-6539/99/0507-2122 $ 17.50+.50/0 *Chem. Eur. J.* **1999**, *5*, No. 7

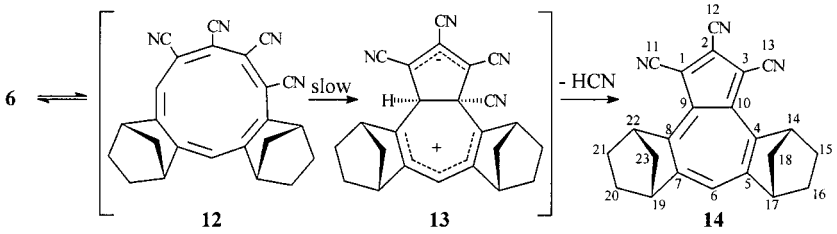

Scheme 3. Reaction scheme for the formation of **14**.

The dark blue color of **6** is surprising, because the two isolated substituted 1,3-cyclohexadiene chromophores should absorb only ultraviolet light, as they do in the case of the other 9,10-dihydronaphthalene derivatives.[11, 12] From the UV/visible spectrum of 5,5-dichloro-1,2,3,4-tetracyano-1,3-cyclopentadiene ($\lambda_{max} = 338$ nm, $\log \varepsilon = 3.53$) the isolated chromophore 1,2,3,4-tetracyano-1,3-cyclohexadiene is expected to absorb only ultraviolet light.[16] Since the molar extinction coefficients ε are not concentration dependent, we assume that the color of **6** comes from a charge-transfer (CT) band that results from the intramolecular interaction of the relatively electron-rich tetraalkyl-substituted cyclohexadiene moiety with the electron-poor tetracyano-substituted cyclohexadiene moiety. The observed negative solvatochromism of the CT band (the blue shift of the CT absorption maximum caused by the change from the less polar solvent such as CH_2Cl_2 to the more polar solvent acetonitrile, Table 3), shows the same trend as that of the intermolecular tetracyanobenzene/arene charge-transfer complex observed by Hubig and Kochi[17] and may be explained accordingly by means of Marcus theory and the solvent-continuum model.[18] Alternatively, the absorption of visible light may also be the result of the photochemical excitation of a conjugated valence-bond isomer such as **12**, whose equilibrium concentration is below the limits of NMR detection.

Table 3. Solvent dependence of λ_{max} ($\log \varepsilon$) in the UV/Vis spectrum of **6**.

CH_3OH	C_2H_5OH	CH_3CN	CH_2Cl_2	C_6H_6
267 (3.83)	–	263 (4.02)	–	–
281 (3.86)	280 (3.90)	–	280 (3.99)	280 (3.96)
305s (3.71)	–	307 (4.09)	–	–
339 (3.60)	341 (3.60)	337 (3.72)	340 (3.67)	330 (3.66)
–	384 (3.57)	368s (3.42)	–	–
399 (3.52)	399 (3.58)	399 (2.74)	395 (1.75)	–
545 (2.66)	547 (2.59)	539 (2.97)	575 (2.77)	573 (2.76)

Reactions of DCA with benzo[1,2:4,5]dicyclobutene 15 and 5,7,12,14-tetrahydro-5,14:7,12-dimethanopentacene 18: The reaction of DCA with the strained arene derivatives **15** and **18** were investigated with the objective to find out whether the cycloaddition of DCA proceeds to the 1,4 position of the benzene unit of **15** and **18** in a similar fashion to that of octahydrodimethanoanthracene **3**. It is interesting to note that durene, a tetraalkylated benzene derivative with similar substitution patterns to **3**, **15**, or **18**, reacts with DCA to form the symmetrical (1:1) Diels–Alder adduct.[19] In the case of **18** the cycloaddition of DCA to the central benzene ring can compete with those to the terminal benzene rings. As **15** and **18** show similar reactions to **3**, it is interesting to synthesize and investigate the correspondingly substituted COT and 9,10-dihydronaphthalene derivatives that have more rigid torsional constraints than **7** or **6**. At 1 bar and 125 °C **15**[20] reacts with DCA to give the benzocyclobutene derivative **17** as the only product. At 11 kbar the reaction between DCA and **15** occurs readily at 53 °C producing the Diels–Alder adduct **16** besides **17** (Scheme 4). The Diels–Alder adduct **16**, separated from its isomer **17** by liquid chromatography, is thermally labile and undergoes an intramolecular *retro*-Diels–Alder reaction to give **17** on heating at 53 °C (half-life: 2.5 h). Attempts to catalyze the cycloaddition of DCA to **15** by means of a Lewis acid, such as $AlCl_3$ or $TiCl_4$, failed. The reaction of DCA with **15** in the presence of $AlCl_3$ or $TiCl_4$ leads to products of higher molecular weight that could not be identified. In the photolysis of **16** under conditions comparable with that of **5** only polymers and not the expected COT derivative **10** were formed. The reaction of DCA with **15** demonstrates again that pressure is a useful parameter to control consecutive reactions. The cycloaddition in the first step is accelerated by pressure, whereas the rearrangement (retro-Diels–Alder reaction) in the second step is much less affected by pressure so that the primary adduct **16** (not detectable at atmospheric pressure) can be isolated from the high-pressure reaction.

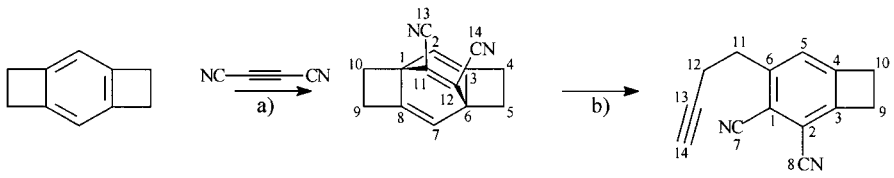

Scheme 4. Addition of DCA to benzodicyclobutene **15**. a) 1 bar, 125 °C, 17 h, **15** and **17** formed in the ratio 46:54 (^{1}H NMR), yield: 39% of **17** (colorless crystals, m.p. 108 °C); 11 kbar, 53 °C, 20 h, yield: 7% of **16** (colorless crystals, m.p. 101 °C) and 3% of **17**. b) 1 bar, 53 °C, 5 h, conversion: 75.7%, $k_1 = (7.7 \pm 0.2) \times 10^{-5}\ s^{-1}$, $\Delta G^{\neq} = 24.4$ kcal mol^{-1}).

The utility of high pressure in synthesis can be also demonstrated with the reaction between DCA and tetrahydrodimethanopentacene **18** (Scheme 5).[21] At 1 bar and 130 °C only the (1:1) Diels–Alder adduct **19** is formed, whereas at 12 kbar the reaction between DCA and **18** occurs at 50 °C producing in addition to **19** the adducts **20**, as colorless crystals, and **21**, as a green-blue amorphous solid. The 9,10-dihydronaphthalene derivative **21** undergoes a rapid degenerate rearrangement on the NMR time scale at room temperature, analogous to that of **6**. The activation parameters were again determined from the analysis of the

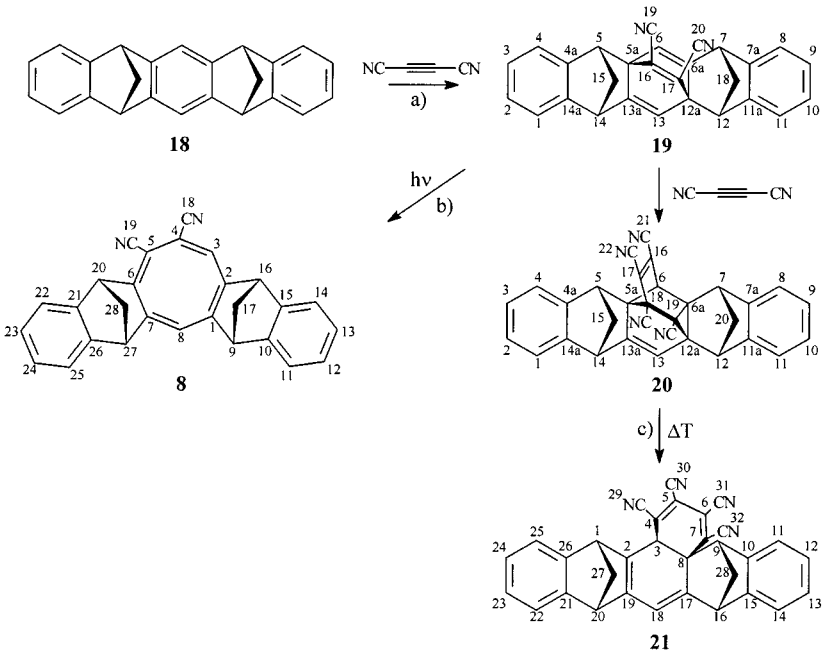

Scheme 5. Addition of DCA to tetrahydrodimethanopentacene **18**. a) 1 bar, 130 °C, 41 h, conversion: 58 %, yield: 22 % of **19**; 12 kbar, 50 °C, 44 h, conversion: 75 %, yield: 32 % of **19**, 1.5 % of **20** (colorless crystals) and 3 % of **21** (green-blue crystals). b) *hν* (300 nm), 35 min, hexane, acetone (10:1), yield: 69 % of **8** (red-brown amorphous solid, m.p. 115 °C). c) 1 bar, 55 °C, 6 h, conversion: 73.2 %, $k_1 = (6.5 \pm 1.1) \times 10^{-5}\ s^{-1}$, $\Delta G^{\neq} = 24.6\ kcal\,mol^{-1}$).

temperature-dependent line shape of the exchanging ^1H NMR signals: $\Delta H^{\neq} = (9.6 \pm 0.5)\ kcal\,mol^{-1}$, $\Delta S^{\neq} = -(5 \pm 2)\ cal\,mol^{-1}\,K^{-1}$, and $\Delta G^{\neq} = (10.7 \pm 0.7)\ kcal\,mol^{-1}$ at $-60\,^{\circ}C$ in CD_2Cl_2; these values are in good agreement with those determined for the degenerate rearrangement in **6** (Table 2). Evidently, the replacement of the ethano bridges in **6** by the more rigid benzo groups in **21** has no significant effect on the structure and degenerate rearrangement of the 9,10-dihydronaphthalene unit incorporated in both systems. Photolysis of the (1:1) adduct **19** leads to the red-brown COT derivative **8**, whose spectral properties agree very well with those of the corresponding COT derivative **7**. Since no crystals suitable for a crystal structure analysis could be grown to date, the question remains open, whether the more rigid torsional constraints in **8** caused by the benzo substitution lead to a further planarization of the eight-membered ring.

Density functional theory calculations of the degenerate [1,5] vinyl shift: The degenerate rearrangement of **6** is formally a sigmatropic [1,5] vinyl shift.[22] It may occur through an orbital-symmetry-allowed concerted pathway. Alternatively, stepwise diradical or zwitterionic processes are possible. We have examined the mechanism of the [1,5]-shift reactions of **6** (R = CN), and also of a model system, **24** (R = H), at the Becke3LYP/6-31G* hybrid HF-DFT level (Scheme 6); this gives excellent energetics for both concerted and stepwise diradical mechanisms of other pericyclic reactions,[23] including Diels–Alder reactions[24] and [1,3] sigmatropic shifts.[25] The method also gives excellent geometries for transition structures of pericyclic reactions as shown by comparison of predicted kinetic isotope effects to high-precision experimental results.[26]

Computational methodology: All calculations were performed with Gaussian 94 at the Becke3LYP/6-31G* level.[27, 28] All geometries were fully optimized. Owing to the prohibitive computational cost, vibrational frequency calculations were not carried out. Restricted and unrestricted Becke 3LYP/6-31G* were used for closed-, and open-shell species, respectively. Energies are not corrected for zero-point vibrational energy (ZPE).

The [1,5] sigmatropic shift of model system **24** (R = H) is predicted to occur through a stepwise mechanism. The Becke 3LYP/6-31G* optimized geometries of the reactant **24**, transition structure **25**$^{\neq}$, and intermediate **26** are shown in Figure 5. The geometries of both **25**$^{\neq}$ and **26** were optimized with unrestricted DFT (UBecke 3LYP), and that of **24** was obtained with restricted DFT (RBecke3LYP). Bond formation in transition structure **25**$^{\neq}$ is advanced; the forming C–C bond length is 1.927 Å. Conversely, the C–C bond which is broken during the reaction is stretched by only 0.07 Å in the transition structure. The lengths of the forming and breaking C–C bonds are similar to those found in the transition structure for the [5,5] sigmatropic rearrangement of (*Z*,*Z*)-1,3,7,9-decatetraene, a reaction which is predicted to occur by a diradical mechanism at the same level of theory.[29]

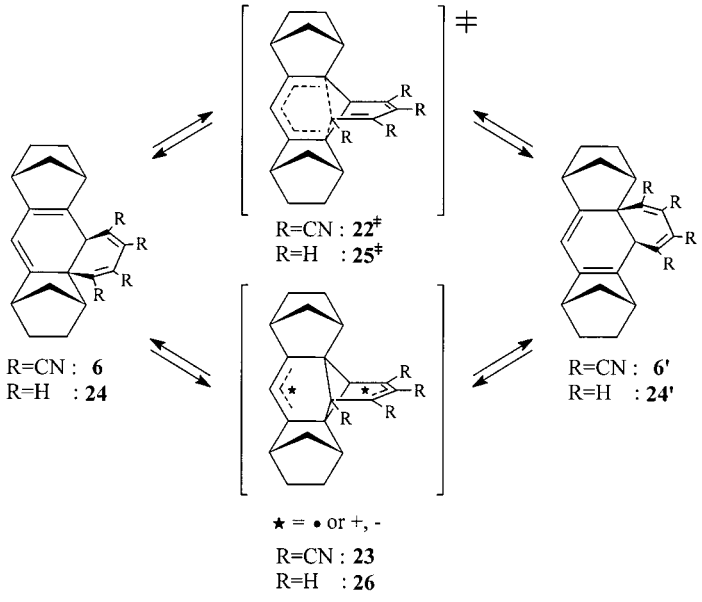

Scheme 6. Potential mechanisms of the degenerate rearrangements **6** ⇌ **6′** and **24** ⇌ **24′**.

0947-6539/99/0507-2124 $ 17.50+.50/0 *Chem. Eur. J.* **1999**, *5*, No. 7

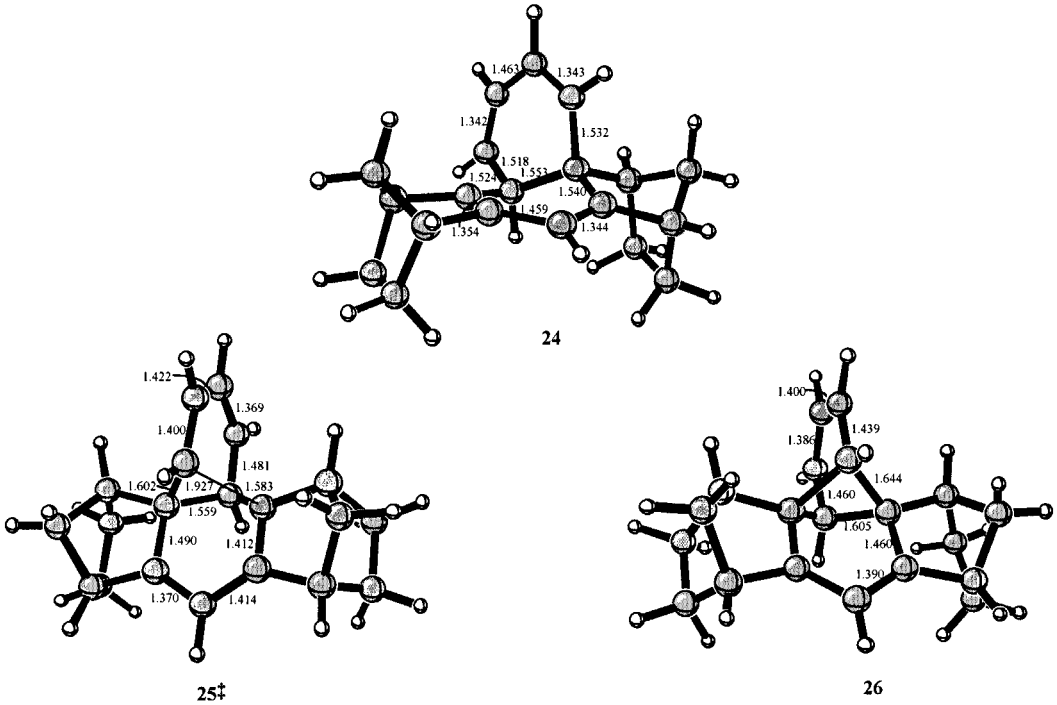

Figure 5. Becke3LYP/6-31G* reactant **24**, transition structure **25**$^{\pm}$, and intermediate **26** for the [1,5]-sigmatropic-shift model system. All bond lengths are in Å.

Intermediate **26** is formed via the transition structure **25**$^{\pm}$ with a predicted $\Delta E^{\pm}$ of 20.8 kcal mol^{-1}. The formation of **26** is endothermic by 18.5 kcal mol^{-1}. The bonds that are formed and broken during the reaction are both 1.644 Å in length in the intermediate, and the species has approximately C_s symmetry with two allyl moieties. Both zwitterionic and diradical stepwise mechanisms are possible, though a diradical mechanism should be favored in the gas phase. The $\langle S^2O \rangle$ values for **25**$^{\pm}$ and **26** are both 0.0. The complete lack of spin-contamination suggests that the structures are closed-shell singlets, which would be expected for a zwitterionic mechanism. The Becke3LYP/6-31G* optimized reactant **6**, transition structure **22**$^{\pm}$, and intermediate **23** for the [1,5] sigmatropic shift of **6** are shown in Figure 6. Both **22**$^{\pm}$ and **23** were located at the UBecke3LYP/6-31G* level, and the geometry of **6** was optimized at the RBecke3LYP/6-31G* level.

Like the [1,5] shift of model system **24**, the reaction of **6** is predicted to occur by a stepwise mechanism. The geometry of transition structure **22**$^{\pm}$ is similar to that of **25**$^{\pm}$. However, **22**$^{\pm}$ occurs slightly earlier on the reaction pathway. The length of

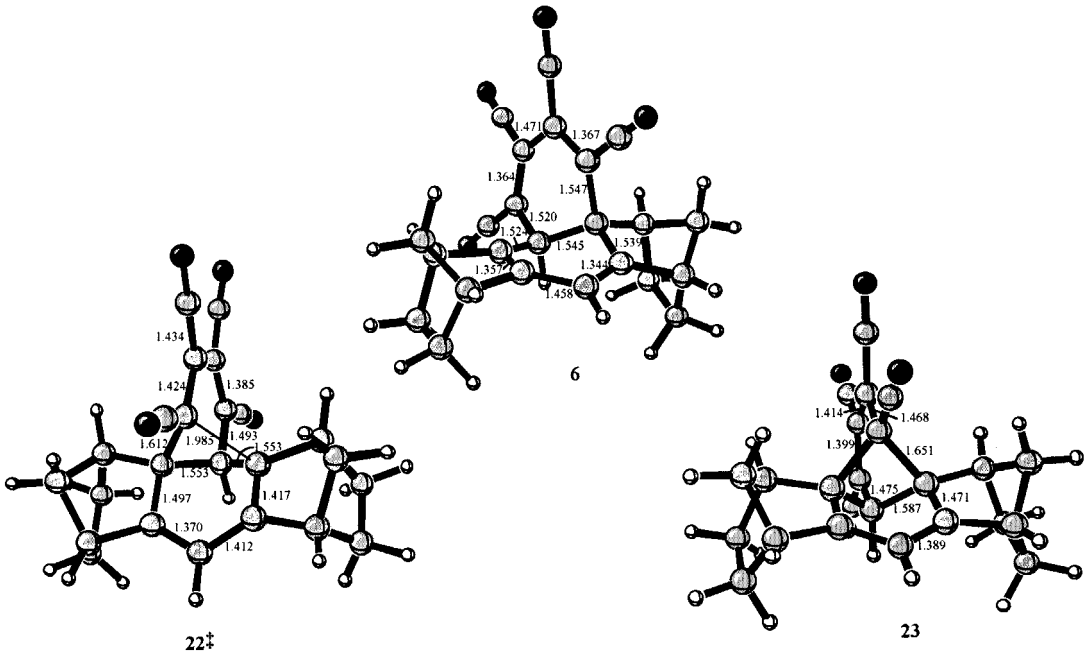

Figure 6. Becke3LYP/6-31G* reactant **6**, transition structure **22**$^{\pm}$, and intermediate **23** for the [1,5] sigmatropic shift. All bond lengths are in Å.

the forming C–C bond in **22**‡ is 1.985 Å, compared with a forming C–C bond length of 1.927 Å in **25**‡. In addition, the breaking C–C bond in **22**‡ is stretched to a smaller extent than the corresponding C–C bond in **25**‡. Intermediate **23** is formed via the transition structure **22**‡ with a predicted $\Delta E^{\ddagger}$ of 12.5 kcal mol^{-1}, while the $\Delta E_{rxn.}$ for the formation of **23** is only 9.5 kcal mol^{-1}. The DFT $\Delta E^{\ddagger}$ is in good agreement with the experimental $\Delta H^{\ddagger}$ ($-60\,^{\circ}$C, MeOH) of 12.0 ± 0.4 kcal mol^{-1}. In the gas phase, a diradical mechanism for the [1,5] shift of **6** should be more favorable than a zwitterionic mechanism. However, the $\langle S^2O \rangle$ values in UB3LYP calculations for **22**‡ and **23** are also both 0.0, indicative of no diradical character. Even in the gas phase calculations, the Becke3LYP dipole moments for **6**, **22**‡, and **23** are 8.2, 10.4, and 11.0 Debye, respectively (Table 4). Intermediate **23** and transition structure **22**‡ are both even more polar than reactant **6**. The gas-phase energy of **23** is also only 9.5 kcal mol^{-1} above **6**. As solvent polarity increases, intermediate **23** will be stabilized to a much larger extent than **6**. If this differential stabilization is large enough, **23** could become the more stable species. This would lead to an increase in the measured activation barrier, which could explain the experimental observations. However, from the observation of the spectral properties of **6**, compound **23** is not the ground state of the equilibrating system **6** $\rightleftharpoons$ **6′** in methanol. Therefore, the effect of solvation on the stabilities of **6** and **23** is currently being evaluated with SCIPCM single-point calculations.

Table 4. Energies [Hartrees], dipole moments [Debye], and $\langle S^2O \rangle$ for **6** and **22**–**26**.

	Energy	μ	$\langle S^2O \rangle$
6	–1144.24477	8.2	0.0
24	–775.28878	0.6	0.0
25	–775.25570	0.6	0.0
26	–775.25925	0.7	0.0
22	–1144.22510	10.4	0.0
23	–1144.22958	11.0	0.0

Conclusion

The reactions of DCA with the partially hydrogenated dimethanoanthracene or pentacene derivatives **3** and **18** lead to the (1:1) Diels–Alder adducts **5** and **19**, respectively, and to the 9,10-dihydronaphthalene derivatives **6** or **21**, both of which are intensely colored—most likely due to a charge-transfer absorption of visible light. Photolysis of the (1:1) adducts **5** and **19** produces the corresponding cyclooctatetraene derivatives **7** and **8**, which are not planar despite the torsional constraints contrary to the predictions from molecular-model considerations,[1] but in agreement with semi-empirical quantum mechanical calculations. The mechanism of formation of the dihydronaphthalene derivatives **6** and **21** could be elucidated by the use of high pressure; this allowed the (2:1) adducts **11** and **20** to be detected as intermediates in the reactions of DCA with **5** or **19** leading to **6** and **21**, respectively. A degenerate rearrangement consisting formally of a [1,5] vinyl shift in **6** and **21** could be detected with the temperature dependence of their ^{1}H NMR spectra. The mechanisms of these [1,5]-sigmatropic-shift reactions of **6** and **24** have been examined at the Becke3LYP/6-31G* level of theory. Stepwise mechanisms are predicted, and the transition structure **22**‡ and the intermediate **23** are calculated to be more polar than the starting material **6**. The gas-phase activation barrier calculated for the [1,5] shift of **6** is in good agreement with the measured $\Delta H^{\ddagger}$ in solution. The finding that the irreversible rearrangement of **6** accompanied by the elimination of HCN to give the azulene derivative **14** proceeds only on heating of **6** to 80 °C in a polar solvent is a good evidence for the polar mechanism for this reaction.

Experimental Section

IR: Perkin-Elmer FTIR 1600. UV: Perkin-Elmer Lambda 9. ^{1}H NMR, ^{13}C NMR, DEPT and two dimensional experiments (H,H-COSY, C,H-COSY, NOESY, HMQC and HMBC): Bruker AMX 300; the undeuterated amount of the solvent was used as an internal standard; x is used for *exo* and n is used for *endo*. MS: Fison Instruments VG ProSpec 3000 (70 eV). GLC-MS: Hewlett-Packard 5971 A MSD (70 eV), quartz capillary column OV 1 (50 m). GLC: Carlo Erba Strumentazione, quartz capillary column OV 17 (25 m). Crystal structure analysis: Siemens P4-diffractometer, Siemens SMART-CCD-diffractometer. Column chromatography: Roth silicagel 0.063–0.2 mm. TLC: Macherey & Nagel Kieselgel Fertigplatten Polygram SIL-G/UV$_{254}$. All melting points are uncorrected. Ampoules were sealed in vacuo after two freeze (*iso*-propanol/dry ice) and thaw cycles using argon as an inert gas. High-pressure equipment (up to 14 kbar): A. W. Birks, Department of Mechanical and Industrial Engineering at the Queen's University of Belfast; A. Hofer Mülheim, Ruhr. General procedure for high-pressure reactions: In the autoclave filled with pressure-transducing medium the sealed PTFE-tube containing the reaction solution was pressurized to 5 kbar, then heated to the reaction temperature and finally pressurized to the desired pressure.

1,2,3,4,5,6,7,8,8a,9,10,10a-Dodecahydro-1,4:5,8-dimethanoanthracene (*endo,exo*-2)

A) at 1 bar: A mixture of norbornene (11.7 g, 0.12 mol) and 2,3-bis-*exo*-methylenenorbornane (2.15 g, 18 mmol)[5] was heated in a sealed ampoule at 160 °C for 22 h. The excess of norbornene was removed by vacuum distillation. GLC-analysis of the residue showed an *endo,exo*-**2**/*endo,endo*-**2** ratio of 88:12. Repeated recrystallization (twice) at $-20\,^{\circ}$C from ethanol gave 1.85 g of colorless crystals of *endo,exo*-**2** (yield: 50 %).

B) at 7.9 kbar: A solution (100 µL) containing 2,3-bis-*exo*-methylenenorbornane (95 mg, 0.8 mmol), norbornene (500 mg, 5.32 mmol), and *n*-dodecane (113 mg) as internal standard in toluene (2.5 g) sealed in a PTFE-tube was heated to 75 °C for 6 h at a pressure of 7.9 kbar. GLC analysis showed a conversion of 30 % and an *endo,exo*-**2**/*endo,endo*-**2** ratio of 96:4. M.p. 35 °C; ^{1}H NMR (300 MHz, $CDCl_3$): $\delta = 0.85$ (m, 2H; 2-H$_n$, 3-H$_n$), 0.95 (m, 2H; 11-H$_x$, 12-H$_x$), 1.12 (m, 2H; 6-H$_n$, 7-H$_n$), 1.25 (m, 1H; 11-H$_n$), 1.45–1.55 (m, 7H; 2-H$_x$, 3-H$_x$, 6-H$_x$, 7-H$_x$, 8a-H, 10a-H, 12-H$_n$), 1.68 (m, 2H; 9-H$_n$, 10-H$_n$), 1.88 (m, 2H; 5-H, 8-H), 2.25 (m, 2H; 9-H$_x$, 10-H$_x$), 2.65 (m, 2H; 1-H, 4-H); ^{13}C NMR (75 MHz, $CDCl_3$): $\delta = 25.75$ (C-2, C-3), 28.43 (C-9, C-10), 29.83 (C-6, C-7), 33.61 (C-12), 44.40 (C-8a, C-10a), 44.43 (C-5, C-8), 45.78 (C-1, C-4), 46.54 (C-11), 139.63 (C-4a, C-9a); IR (KBr): $\tilde{\nu} = 2949$ (CH), 2864 cm^{-1} (CH); MS (70 eV), *m*/*z* (%): 214 (17) [M^+], 186 (100) [$M^+ - C_2H_4$].

1,2,3,4,5,6,7,8-Octahydro-1,4:5,8-dimethanoanthracene (3): A solution of DDQ (670 mg, 3 mmol) in toluene (5 mL) was added to a solution of *endo,exo*-**2** (260 mg, 1.2 mmol) in toluene (2 mL), and the deep red mixture is stirred at 80 °C for 2 h. The reaction mixture is purified by column chromatography (30 g silica gel, hexane). Yield of **3**: (255 mg, > 99 %) as colorless crystals; m.p. 117 °C; ^{1}H NMR (300 MHz, $CDCl_3$): $\delta = 1.13$ (m, 4H; 2-H$_n$, 3-H$_n$, 6-H$_n$, 7-H$_n$), 1.46 (m, 2H; 11-H$_x$, 12-H$_x$), 1.70 (m, 2H; 11-H$_n$, 12-H$_n$), 1.83 (m, 4H; 2-H$_x$, 3-H$_x$, 6-H$_x$, 7-H$_x$), 3.23 (s, 4H; 1-H, 4-H, 5-H,

0947-6539/99/0507-2126 $ 17.50+.50/0 *Chem. Eur. J.* **1999**, *5*, No. 7

8-H), 6.95 (s, 2H; 9-H, 10-H); ^{13}C NMR (75 MHz, $CDCl_3$): $\delta = 27.24$ (C-2, C-3, C-6, C-7), 43.58 (C-1, C-4, C-5, C-8), 49.75 (C-11, C-12), 113.33 (C-9, C-10), 145.20 (C-4a, C-8a, C-9a, C-10a); IR (KBr): $\tilde{\nu} = 2980$ (CH), 2967 (CH), 2860 cm^{-1} (CH); UV/Vis (CH_3CN): λ_{max} ($\log\varepsilon$) = 230 (3.64), 277 (3.58), 282 nm (3.54); MS (70 eV): *m/z* (%): 210 (37) [M^+], 182 (100) [$M^+ - C_2H_4$], 154 (88) [$M^+ - 2C_2H_4$]; $C_{16}H_{18}$: calcd 210.1409, found 210.1408 (MS).

4a,9a-Epoxy-1,2,3,4,4a,5,6,7,8,8a,9,9a,10,10a-tetradecahydro-1,4:5,8-dimethanoanthracene (4):

Method A: A solution of *m*-chloroperoxybenzoic acid (670 mg, 70%, 2.7 mmol) in CH_2Cl_2 (7 mL) was added to a solution of *endo,exo*-**2** (572 mg, 2.65 mmol) in CH_2Cl_2 (5 mL) at 0 °C. The mixture was stirred at 5 °C for 16 h. The solution was diluted with CH_2Cl_2 (20 mL) and washed with NaOH (1M, 2 × 10 mL) and water (10 mL). The solution was dried over Na_2SO_4 and filtered. After evaporation of the solvent 490 mg of **4** (2.1 mmol, yield: 80%) was obtained as colorless crystals.

Method b): A stream of air saturated with CH_2Cl_2 was bubbled through a glass tube into the refluxing solution of *endo,exo*-**2** (216 mg, 1 mmol) in CH_2Cl_2 (4 mL) for 24 h. After evaporation of the solvent in vacuo the residue is purified by column chromatography on silica gel (100 g, hexane/ethyl acetate 10:1). Yield: 100 mg of **4** (44%); m.p. 119 °C; ^{1}H NMR (300 MHz, $CDCl_3$): $\delta = 0.55$ (m, 1H; 15-H_x), 0.92 (m, 1H; 16-H_x), 1.12 (m, 4H; 3-H_x, 10-H_x, 6-H_n, 7-H_n), 1.3–1.5 (m, 8H; 6-H_x, 7-H_x, 13-H_x, 13-H_n, 14-H_x, 14-H_n, 15-H_n, 16-H_n), 1.55 (m, 2H; 4-H, 9-H), 1.76 (m, 2H; 5-H, 8-H), 2.20 (m, 2H; 3-H_n, 10-H_n), 2.35 (m, 2H; 1-H, 12-H); ^{13}C NMR (75 MHz, $CDCl_3$): $\delta = 24.35$ (C-13, C-14), 28.28 (C-3, C-10), 29.61 (C-6, C-7), 30.87 (C-15), 32.11 (C-16), 41.69 (C-1, C-12), 41.87 (C-4, C-9), 43.43 (C-5, C-8), 57.67 (C-2, C-11); IR (KBr): $\tilde{\nu} = 2950$ (CH), 2874 (CH), 1196 cm^{-1} (C–O).

Addition of dicyanoacetylene to 3

A) at 1 bar: A solution of **3** (420 mg, 2 mmol) and dicyanoacetylene (200 mg, 2.6 mmol) in benzene (3 mL) was heated in a sealed ampoule at 127 °C for 17 h. After evaporation of the solvent in vacuo, the dark blue residue showed a composition of **3**:**5**:**6** = 30:56:14 (^{1}H NMR analysis). The mixture was separated by column chromatography on silica gel (50 g, hexane/ethyl acetate 10:1). 1st fraction: **3** (120 mg), 2nd fraction: 280 mg of **5** (yield: 49%) colorless crystals, and 3rd fraction: 50 mg of **5** (yield: 11%) dark blue crystals.

B) at 9 kbar: A solution of **3** (84 mg, 0.4 mmol) and dicyanoacetylene (50 mg, 0.65 mmol) in toluene (1 mL) was heated in a sealed PTFE tube to 83 °C for 17 h at a pressure of 9 kbar. After evaporation of the solvent in vacuo, the black residue showed a composition of **3**:**5**:**6** = 64:13:23 (^{1}H NMR analysis). Work-up analogous to a) leads to 27 mg of **3**, 9 mg of **5** (yield: 8%), and 33 mg of **6** (yield: 28%).

Compound 5: M.p. 192 °C; ^{1}H NMR (300 MHz, $CDCl_3$): $\delta = 1.20$ (m, 2H; 6-H_n, 13-H_n), 1.55–1.8 (m, 10H; 6-H_x, 7-H_x, 7-H_n, 13-H_x, 14-H_x, 14-H_n, 15-H, 18-H), 2.85 (m, 2H; 5-H, 12-H), 3.1 (m, 2H; 1-H, 8-H), 6.0 (s, 2H; 3-H, 10-H); ^{13}C NMR (75 MHz, $CDCl_3$): $\delta = 24.26$ (C-7, C-14), 28.07 (C-6, C-13), 38.60 (C-1, C-8), 38.72 (C-5, C-12), 41.34 (C-15, C-18), 69.48 (C-2, C-9), 113.12 (C-19, C-20), 121.11 (C-3, C-10), 141.47 (C-16, C-17), 164.91 (C-4, C-11); IR (KBr): $\tilde{\nu} = 2965$ (CH), 2909 (CH), 2872 (CH), 2210 cm^{-1} (C≡N); UV/Vis (CH_3OH): λ_{max} ($\log\varepsilon$) = 242 (3.70), 249 (3.67), 345 nm (2.54); MS (70 eV): *m/z* (%): 286 (100) [M^+], 258 (67) [$M^+ - C_2H_4$], 230 (50) [$M^+ - 2C_2H_4$]; $C_{20}H_{18}N_2$: calcd 286.1470, found 286.1459 (MS).

Compound 6: M.p. 159 °C (decomp); ^{1}H NMR (300 MHz, CD_2Cl_2, −80 °C): $\delta = 0.76–1.88$ (m, 12H; 4-H, 5-H, 11-H, 12-H, 19-H, 20-H), 2.36 (m, 1H; 3-H), 2.69 (m, 1H; 13-H), 2.93 (m, 1H; 6-H), 3.09 (m, 1H; 10-H), 3.50 (s, 1H; 1-H), 6.12 (s, 1H; 8-H); ^{1}H NMR (300 MHz, $CDCl_3$, 20 °C): $\delta = 1.10$ (m, 2H; 4-H_n, 12-H_n), 1.2–1.35 (m, 4H; 5-H_n, 11-H_n, 19-H_x, 20-H_x), 1.5–1.8 (m, 6H; 19-H_n, 20-H_n, 4-H_x, 5-H_x, 11-H_x, 12-H_x), 2.6 (m, 2H; 3-H, 13-H), 3.05 (m, 2H; 6-H, 10-H), 3.45 (s, 1H; 1-H), 6.1 (s, 1H; 8-H); see also Table 5; ^{13}C NMR (75 MHz, $CDCl_3$): $\delta = 23.21$ (C-4, C-12), 27.25 (C-5, C-11), 39.62 (C-1), 40.03 (C-19, C-20), 42.26 (C-6, C-10), 43.37 (C-3, C-13), 113.47 (C-2, C-14), 114.29 (C-8), 146.04 (C-7, C-9), 110.03, 110.07, 113.53, 116.36, 117.70, 128.94, 137.86 (C-15, C-16, C-17, C-18, C-21, C-22, C-23, C-24); IR (KBr): $\tilde{\nu} = 2967$ cm^{-1} (CH), 2217 cm^{-1} (C≡N); UV/Vis (CH_3OH): λ_{max} ($\log\varepsilon$) = 267 (3.83), 281 (3.86), 305 (3.71), 339 (3.60), 399 (3.52), 545 nm (2.66); MS (70 eV): *m/z* (%): 362 (26) [M^+], 334 (100) [$M^+ - C_2H_4$], 306 (42) [$M^+ - 2C_2H_4$]; $C_{24}H_{18}N_4$: calcd 362.1531, found 362.1554 (MS).

Table 5. Specific rate constants *k* of the degenerate rearrangement of **6** determined by line-shape analysis of the signals at $\delta = 2.67$ and 2.99 in CD_3OD and 2.60 and 3.08 in CD_2Cl_2, assigned to 3-H, 13-H and 6-H, 10-H, respectively, and $\delta = 2.47$ in [D_8]toluene, assigned to 6-H, 10-H, in the temperature-dependent ^{1}H NMR spectra of **6**.

in CD_3OD		in CD_2Cl_2		in [D_8]toluene	
T [°C]	*k* [s^{-1}]	*T* [°C]	*k* [s^{-1}]	*T* [°C]	*k* [s^{-1}]
−20	2500	−40	800	−40	475
−40	200	−65	100	−50	299.4
−45	120	−70	75	−60	135.3
−50	52	−80	20	−70	42.7
−55	32			−80	17.1
−65	10				
−80	1				

Photolysis of 5

Method A: A solution of **5** (440 mg, 1.54 mmol) in acetone (37 mL) was diluted with hexane (370 mL) and divided into 80 mL portions. Each portion degassed with Argon was filled in a 100 mL ampoule (pyrex, ∅ = 3 cm). Each ampoule was placed in a water cooled quartz photolysis vessel and irradiated with sixteen 300 nm lamps (25 W) in a Rayonet reactor for 45 min. The combined orange photolyzed solutions were concentrated in vacuo. The residue, consisting of a red-brown oil, was dissolved in CH_2Cl_2 (2 mL). The addition of hexane (5 mL) lead to the formation of a second layer. Compound **7** crystallized during the slow diffusion of hexane into the CH_2Cl_2 layer. Yield: 300 mg of **7** (68%) red-orange crystals.

Method B: A solution of **5** (30 mg, 0.1 mmol) in acetone (30 mL) was irradiated in analogy to method A. After 30 min **5** had completely disappeared and only **7** was detected by TLC and ^{1}H NMR analysis.

Compound 7: M.p. 151 °C; ^{1}H NMR (300 MHz, $CDCl_3$): $\delta = 0.85$ (m, 2H; 10-H_n, 11-H_n), 1.1 (m, 1H; 13-H_x), 1.25 (m, 3H; 17-H_n, 20-H_n, 20-H_x), 1.6 (m, 5H; 10-H_x, 11-H_x, 13-H_n, 18-H_n, 18-H_x), 1.85 (m, 1H; 17-H_x), 2.55 (m, 1H; 9-H), 2.73 (m, 1H; 12-H), 2.77 (m, 1H; 19-H), 3.45 (m, 1H; 16-H), 5.70 (s, 1H; 8-H), 6.4 (s, 1H; 3-H); ^{13}C NMR (75 MHz, $CDCl_3$): $\delta = 24.49$, 24.54, 24.73 (C-10, C-11, C-18), 30.95 (C-17), 37.19 (C-20), 42.39 (C-13), 45.99 (C-12), 48.09 (C-16), 48.17 (C-9), 48.30 (C-19), 101.64 (C-5), 109.65 (C-4), 116.09 (C-15), 116.82 (C-14), 124.65 (C-8), 144.35 (C-2), 149.13 (C-3), 151.77 (C-1), 152.62 (C-7), 173.17 (C-6); IR (KBr): $\tilde{\nu} = 2963$ (CH), 2941 (CH), 2870 (CH), 2213 (C≡N), 1636 (C=C), 1595 cm^{-1} (C=C); UV/Vis (CH_3OH): λ_{max} ($\log\varepsilon$) = 207 (4.16), 235 (4.31), 256 (4.36), 420 nm (2.51); MS (70 eV): *m/z* (%): 286 (100) [M^+], 258 (77) [$M^+ - C_2H_4$], 230 (63) [$M^+ - 2C_2H_4$]; $C_{20}H_{18}N_2$: calcd 286.1470, found 286.1498.

Addition of dicyanoacetylene to 5

A) at 1 bar: A solution of **5** (80 mg, 0.28 mmol) and dicyanoacetylene (100 mg, 1.3 mmol) in benzene (1 mL) was heated in a sealed ampoule at 127 °C for 17 h. After distillation of the reaction mixture in vacuo, the dark blue residue consisted of **5** and **6** in a ratio of 42:58 (^{1}H NMR analysis). The mixture was separated by column chromatography on silica gel (20 g, hexane/ethyl acetate 10:1). 1st fraction: **5** (30 mg), 2nd fraction: 46 mg of **6** (yield: 45%) dark blue colored crystals.

B) at 12 kbar: A solution of **5** (100 mg, 0.35 mmol) and dicyanoacetylene (50 mg, 0.65 mmol) in toluene (2 mL) was sealed in a PTFE tube and pressurized to 12 kbar for 90 h at 20 °C. After distillation of the reaction mixture in vacuo at 20 °C the black residue had a composition of **5**:**11**:**6** = 49:40:11 (^{1}H NMR analysis). The mixture was separated by column chromatography on silica gel (30 g, hexane/ethyl acetate 6:1). 1st fraction: **5** (38 mg), 2nd fraction: 11 mg of **6** (yield: 9%), 3rd fraction: 44 mg of **11** (yield: 35%) colorless crystals.

Compound 11: M.p. 126 °C (decomp); ^{1}H NMR (300 MHz, $CDCl_3$): $\delta =$ 1.18 (m, 4H; 11-H_n, 17-H_n, 18-H_n, 20-H_x), 1.46 (m, 2H; 10-H_n, 19-H_x), 1.67 (m, 3H; 10-H_x, 11-H_x, 17-H_x), 1.82 (m, 1H; 18-H_x), 2.14 (dm, ^2J(19-H_x, 19-H_n) = 11 Hz, 1H; 19-H_n), 2.30 (dm, ^2J(20-H_x, 20-H_n) = 12 Hz, 1H; 20-H_n), 2.40 (m, 1H; 1-H), 2.62 (s, 1H; 3-H), 2.69 (m, 1H; 12-H), 2.93 (m, 1H; 9-H), 3.00 (m, 1H; 16-H), 6.30 (s, 1H; 14-H); ^{13}C NMR (75 MHz, $CDCl_3$): $\delta = 24.96$ (C-11), 25.13 (C-17), 27.20 (C-10), 29.08 (C-18), 32.40 (C-20), 32.80 (C-7), 34.95 (C-12), 38.55 (C-1), 38.66 (C-19), 40.59 (C-9), 41.79 (C-16), 48.69 (C-3), 54.49 (C-8), 56.49 (C-6), 59.50 (C-13), 74.74 (C-2), 109.97, 111.38, 112.32 (C-21, C-22, C-23, C-24), 115.83 (C-14), 132.75 (C-5), 137.89 (C-4), 148.97 (C-15); IR (KBr): $\tilde{\nu} = 2965$ (CH), 2222 cm^{-1} (C≡N); MS

(70 eV): *m*/*z* (%): 362 (20) [M^+], 335 (100) [M^+ – HCN], 307 (100) [M^+ – HCN – C_2H_4], 279 (66) [M^+ – HCN – 2 C_2H_4]; $C_{24}H_{18}N_4$: calcd 362.1531, found 362.1496 (MS).

Thermolysis of 11: A solution of **11** (3 mg, 8.3 μmol) and **3** (ca. 0.6 mg) as standard in $CDCl_3$ (0.8 mL) was heated in a sealed NMR tube to 60.0 ± 0.2 °C. The time-dependent progress of the reaction was determined by ^{1}H NMR analysis of the signals at $\delta = 6.30$ and 6.95, which were assigned to **11** and **3**, respectively. The specific rate constant k_1 of the rearrangement **11** →**6** was calculated from the time-dependent decrease of **11** against the internal standard by the use of the kinetic law of irreversible first-order reactions (Table 6).

Table 6. Time dependence of reaction **11** →**6** in $CDCl_3$ at 60.0 °C followed by ^{1}H NMR.[a]

t [s]	0	1800	3000	4200	5400	6600
11 [%]	100	60.2	41.3	27.7	26.2	15.2

[a] $k_1 = (2.74 \pm 0.19) \times 10^{-4}$ s^{-1}; $r = 0.9902$

Thermolysis of 6

Method A: A solution of **6** (25 mg, 69 μmol) in methanol (20 mL) was heated in a sealed ampoule at 100 °C for 3 h. After cooling to 20 °C within 16 h, **14** crystallized from the reaction mixture as red needles. Yield: 12 mg of **14** (52 %).

Method B: Solutions of **6** (each 3 mg, 8.3 μmol) in acetonitrile, methanol, CH_2Cl_2 or toluene (each 2 mL) were sealed in ampoules and were thermolyzed under different conditions: The acetonitrile and methanol solutions at 80 °C for 1 h and the CH_2Cl_2 and toluene solutions at 150 °C for 30 min. Each solution was concentrated in vacuo and the progress of the reaction was analyzed by ^{1}H NMR spectroscopy. In the samples of the acetonitrile and methanol solution the ratio between **6** and **14** was determined to be (68:32) and (70:30), respectively. From these ratios the half-life of **6** at 80 °C was estimated to be 110 min (in acetonitrile) and 120 min (in methanol). In the samples of the CH_2Cl_2 and toluene solution no formation of **14** could be detected even after thermolysis at 150 °C for 30 min.

Compound 14: M.p. > 300 °C; ^{1}H NMR (300 MHz, $CDCl_3$): $\delta = 1.38$ (m, 4 H; 15-H_n, 16-H_n, 20-H_n, 21-H_n), 1.75 (dm, ^2J(18-H_x, 18-H_n) = 9.6 Hz, 2 H; 18-H_x, 23-H_x), 1.96 (dm, 2 H; 18-H_n, 23-H_n), 2.18 (m, 2 H; 16-H_x, 20-H_x), 2.31 (m, 2 H; 15-H_x, 21-H_x), 3.64 (m, 2 H; 17-H, 19-H), 4.99 (m, 2 H; 14-H, 22-H), 8.15 (s, 1 H; 6-H); ^{13}C NMR (75 MHz, $CDCl_3$): $\delta = 25.18$ (C-15, C-21), 26.51 (C-16, C-20), 46.80 (C-14, C-22), 47.82 (C-18, C-23), 48.17 (C-17, C-19), 96.86 (C-1, C-3), 112.55 (C-12), 115.75 (C-11, C-13), 123.99 (C-2), 133.31 (C-6), 136.01 (C-9, C-10), 154.36 (C-5, C-7), 161.06 (C-4, C-8); IR (KBr): $\tilde{\nu} = 2950$ (CH), 2875 (CH), 2216 cm^{-1} (C≡N); UV (CH_3OH): λ_{max} ($\log \varepsilon$) = 263 (4.56), 310 (4.77), 337 (4.05), 367 (3.95), 525 nm (3.58); MS (70 eV): *m*/*z* (%): 335 (100) [M^+], 307 (64) [M^+ – C_2H_4], 279 (59) [M^+ – 2 C_2H_4]; $C_{23}H_{17}N_3$: calcd 335.1422, found. 335.1422 (MS).

Addition of dicyanoacetylene to 15:

A) at 1 bar: A solution of **15** (130 mg, 1 mmol) and dicyanoacetylene (100 mg, 1.3 mmol) in benzene (1.2 mL) was heated in a sealed ampoule at 125 °C for 17 h. After concentration of the reaction mixture in vacuo the brown residue had a composition of **15**:**17** = 46:54 (^{1}H NMR analysis). The mixture was separated by column chromatography on silica gel (20 g, hexane/ethyl acetate 3:1). 1st fraction: **15** (50 mg), 2nd fraction: 80 mg of **17** (yield: 39 %), colorless crystals.

B) at 12 kbar: A solution of **15** (210 mg, 1.61 mmol) and dicyanoacetylene (160 mg, 2.1 mmol) in hexane (3 mL) was heated in a sealed in a PTFE tube to 53 °C for 20 h at 11 kbar. After concentration of the reaction mixture in vacuo a grey residue was obtained. The excess of **15** (160 mg) was removed by sublimation and the residue was separated by column chromatography on silica gel (12 g, hexane/ethyl acetate 10:1). 1st fraction: 24 mg of **16** (yield: 7 %), colorless crystals, 2nd fraction: 9 mg of **17** (yield: 3 %).

Compound 16: M.p. 101 °C; ^{1}H NMR (300 MHz, $CDCl_3$): $\delta = 2.84 - 3.15$ (m, 8 H; 4-H, 5-H, 9-H, 10-H), 6.10 (t, ^4J (2-H, 4-H) = 2.2 Hz, 2 H; 2-H, 7-H); ^{13}C NMR (75 MHz, $CDCl_3$): $\delta = 24.67$, 25.30 (C-4, C-5, C-9, C-10), 66.07 (C-1, C-6), 113.05 (C-13, C-14), 126.96 (C-2, C-7), 135.36 (C-11, C-12), 156.63 (C-3, C-8); IR (KBr): $\tilde{\nu} = 3259$ (C–H), 2922 (C–H), 2208 cm^{-1} (C≡N); UV/Vis (CH_3OH): λ_{max} ($\log \varepsilon$) = 213 (4.00), 251 (3.70), 296 (2.90), 307 (2.90), 334 nm (2.46); MS (70 eV): *m*/*z* (%): 206 (66) [M^+], 167 (100) [M^+ – C_3H_3], 140 (90) [M^+ – C_3H_3 – HCN]; $C_{14}H_{10}N_2$: calcd 206.0844, found. 206.0817 (MS).

Compound 17: M.p. 108 °C; ^{1}H NMR (300 MHz, $CDCl_3$): $\delta = 1.97$ (t, ^4J (12-H, 14-H) = 3 Hz, 1 H; 14-H), 2.54 (td, ^3J (11-H, 12-H) = 6 Hz, 2 H; 12-H), 3.05 (t, 2 H; 11-H), 3.33 (t, 4 H; 9-H, 10-H), 7.33 (s, 1 H; 5-H); ^{13}C NMR (75 MHz, $CDCl_3$): $\delta = 19.61$ (C-12), 29.23 (C-9), 30.15 (C-10), 33.56 (C-11), 70.63 (C-14), 81.58 (C-13), 109.67, 115.10 (C-7, C-8), 113.06 (C-1), 113.66 (C-2), 128.47 (C-5), 145.27 (C-6), 148.92 (C-3), 151.67 (C-4); IR (KBr): $\tilde{\nu} = 3293$ (C≡C–H), 3273 (C≡C–H), 2944 (CH), 2226 cm^{-1} (C≡N); MS (70 eV): *m*/*z* (%): 206 (60) [M^+], 167 (100) [M^+ – C_3H_3], 140 (90) [M^+ – C_3H_3 – HCN]; $C_{14}H_{10}N_2$: calcd 206.0844, found. 206.0843 (MS).

Thermolysis of 16: A solution of **16** (2 mg, 10 μmol) in [D_6]benzene (0.7 mL) was heated in a sealed NMR tube to 53 ± 1 °C. The time-dependent progress of the reaction was determined by ^{1}H NMR analysis of the signals at $\delta = 5.38$ and 6.32 assigned to **16** and **17**, respectively. The specific rate constant k_1 of the rearrangement **16** →**17** was calculated from the time-dependent ratio of **16** and **17**, by the use of the kinetic law of irreversible first-order reactions (Table 7).

Table 7. Time dependence of reaction **16** →**17** in [D_6]benzene at 53 °C followed by ^{1}H NMR.[a]

t [s]	0	10800	14400	18000	22200
16 [%]	100	41.1	31.6	24.3	18.2

[a] $k_1 = (7.7 \pm 0.2) \times 10^{-5}$ s^{-1}; $r = 0.9991$

Addition of dicyanoacetylene to 18:

A) at 1 bar: A solution of **18** (73 mg, 0.24 mmol) and dicyanoacetylene (25 mg, 0.33 mmol) in toluene (3 mL) was heated in a sealed ampoule at 130 °C for 41 h. After concentration of the reaction mixture in vacuo the brown residue was separated by column chromatography on silica gel (20 g, hexane/ethyl acetate 10:1). 1st fraction: 31 mg of **18**, 2nd fraction: 20 mg of **19** (yield: 22 %), colorless crystals.

B) at 12 kbar: A solution of **18** (200 mg, 0.65 mmol) and dicyanoacetylene (100 mg, 1.3 mmol) in toluene (5 mL) sealed in a PTFE tube was heated to 50 °C for 44 h at 12 kbar. After concentration of the reaction mixture in vacuo, the black residue was separated by column chromatography on silica gel (50 g, hexane/ethyl acetate 10:1). 1st fraction: 50 mg of **18**, 2nd fraction: 80 mg of **19** (yield: 32 %), colorless crystals, 3rd fraction: 10 mg of **21** (yield: 3 %), green-blue amorphous solid. The 4th fraction obtained by elution with a more polar solvent (hexane/ethyl acetate 3:1) yielded **20** (yield: 5 mg, 1.5 %) as colorless crystals.

Compound 19: M.p. 216 °C (decomp); ^{1}H NMR (300 MHz, $CDCl_3$): $\delta =$ 2.11 (dt, ^2J(15-H_x, 15-H_n) = 9.9 Hz, ^3J(15-H_x, 5-H) = ^3J(15-H_x, 14-H) = 1.5 Hz, 2 H; 15-H_x, 18-H_x), 2.38 (dt, ^3J(15-H_n, 5-H) = ^3J(15-H_n, 14-H) = 1.6 Hz, 2 H; 15-H_n, 18-H_n), 3.74 (m, 2 H; 7-H, 14-H), 4.01 (m, 2 H; 5-H, 12-H), 5.61 (s, 2 H; 6-H, 13-H), 6.87 (dm, ^3J(1-H, 2-H) = 7.3 Hz, 2 H; 1-H, 8-H), 6.99 (m, ^3J(2-H, 3-H) = 7.7 Hz, ^4J(2-H, 4-H) = 1.2 Hz, 2 H; 2-H, 9-H), 7.07 (m, ^3J(3-H, 4-H) = 7.0 Hz, ^4J(1-H, 3-H) = 1.2 Hz, 2 H; 3-H, 10-H), 7.37 (dm, 2 H; 4-H, 11-H); ^{13}C NMR (75 MHz, $CDCl_3$): $\delta = 44.84$ (C-7, C-14), 45.31 (C-5, C-12), 52.93 (C-15, C-18), 70.26 (C-5a, C-12a), 112.71 (C-19, C-20), 121.61 (C-1, C-8), 122.53 (C-4, C-11), 122.55 (C-6, C-13), 125.98 (C-3, C-10), 127.22 (C-2, C-9), 141.40 (C-16, C-17), 142.51 (C-7a, C-14a), 143.97 (C-4a, C-11a), 159.03 (C-6a, C-13a); IR (KBr): $\tilde{\nu} = 3070$ (CH), 2994 (CH), 2970 (CH), 2213 (C≡N), 753 cm^{-1} (C–H); MS (70 eV): *m*/*z* (%): 382 (100) [M^+], 355 (17) [M^+ – HCN]; $C_{28}H_{18}N_2$: calcd 382.1470, found 382.1458 (MS).

Compound 21: M.p. 239 °C (decomp); ^{1}H NMR (300 MHz, CD_2Cl_2): $\delta =$ 2.20 (dt, ^2J(27-H_x, 27-H_n) = 9.1 Hz, ^3J(27-H_x, 1-H) = ^3J(27-H_x, 20-H) = 1.6 Hz, 2 H; 27-H_x, 28-H_x), 2.34 (dt, ^3J(27-H_n, 1-H) = ^3J(27-H_n, 20-H) = 1.5 Hz, 2 H; 15-H_n, 18-H_n), 2.72 (s, 1 H; 3-H), 3.50 (m, 2 H; 1-H, 9-H), 3.95 (s, 2 H; 16-H, 20-H), 6.28 (s, 1 H; 18-H), 6.98 (m, 4 H; 12-H, 13-H, 23-H, 24-H), 7.10 (m, 2 H; 11-H, 25-H), 7.18 (m, 2 H; 14-H, 22-H); ^{13}C NMR (75 MHz, CD_2Cl_2): $\delta = 44.47$ (C-3), 50.93 (C-16, C-20), 51.66 (C-1, C-9), 58 (C-27, C-28), 111.61, 111.70, 114.55, 115.06 (C-29, C-30, C-31, C-32), 117.60 (C-18), 118.29, 120.14 (C-4, C-5, C-6, C-7), 122.04 (C-14, C-22), 123.05 (C-11, C-25), 126.34 (C-12, C-24), 126.72 (C-13, C-23), 128.70 (C-2, C-8), 139.50 (C-17, C-19), 145.69 (C-10, C-26), 150.21 (C-15, C-21); MS (70 eV):

0947-6539/99/0507-2128 $ 17.50+.50/0 *Chem. Eur. J.* **1999**, *5*, No. 7

Table 8. Specific rate constants k of the degenerate rearrangement of **21** determined by line-shape analysis of the signals at $\delta = 3.50$ and 3.95 assigned to 1-H, 9-H and 16-H, 20-H, respexctively, in the temperature-dependent ^{1}H NMR spectra of **21** in CD_2Cl_2.[a]

T [°C]	−23	−33	−43	−48	−53	−63	−73	−83
k [s^{-1}]	1676	780	310	130	85	23	8	4

[a] At −60 °C: $\Delta H^{\neq} = (9.6 \pm 0.5)$ kcal mol^{-1}, $\Delta S^{\neq} = (-5 \pm 2)$ cal mol^{-1} K^{-1}, $\Delta G^{\neq} = (10.7 \pm 0.7)$ kcal mol^{-1}.

m/z (%): 458 (92) [M^+], 431 (53) [$M^+ -$ HCN], 382 (100) [$M^+ - C_4N_2$]; $C_{32}H_{18}N_4$: calcd 458.1531, found 458.1526 (MS).

Compound 20: ^{1}H NMR (300 MHz, CD_2Cl_2): $\delta = 1.20$ (s, 1H; 6-H), 1.80 (dt, ^2J(20-H$_x$, 20-H$_n$) = 11.6 Hz, ^3J(20-H$_x$, 7-H) = ^3J(20-H$_x$, 12-H) = 1.6 Hz, 1H; 20-H$_x$), 2.07 (dt, ^2J(15-H$_x$, 15-H$_n$) = 10.1 Hz, ^3J(15-H$_x$, 5-H) = ^3J(15-H$_x$, 14-H) = 1.5 Hz, 1H; 15-H$_x$), 2.45 (dt, ^3J(15-H$_n$, 5-H) = ^3J(15-H$_n$, 1H; 14-H) = 1.5 Hz, 15-H$_n$), 2.75 (dt, ^3J(20-H$_n$, 7-H) = ^3J(20-H$_n$, 12-H) = 1.7 Hz, 1H; 20-H$_n$), 3.35 (m, 1H; 5-H), 3.55 (m, 1H; 12-H), 3.82 (m, 1H; 14-H), 3.88 (m, 1H; 7-H), 6.25 (s, 1H; 13-H), 6.85–7.10, 7.30 (m, 8H; 1-H, 2-H, 3-H, 4-H, 8-H, 9-H, 10-H, 11-H); ^{13}C NMR (75 MHz, CD_2Cl_2): $\delta = 42.68$ (C-12), 43.66 (C-20), 45.73 (C-5), 46.10 (C-19), 47.82 (C-7), 48.78 (C-14), 50.21 (C-15), 52.95 (C-6), 58.53 (C-18), 59.05 (C-6a), 65.01 (C-11a), 75.89 (C-5a), 110.60, 111.63, 112.37, 115.92 (C-21, C-22, C-23, C-24), 118.10 (C-13), 121.68, 122.42, 122.54, 123.09, 126.31, 126.67, 126.79, 127.81 (C-1, C-2, C-3, C-4, C-8, C-9, C-10, C-11), 132.45 (C-17), 139.17 (C-16), 143.71 (C-4a), 144.98 (C-13a), 145.96 (C-14a), 146.23 (C-11a), 147.90 (C-7a).

Photolysis of 19: A solution of **19** (80 mg, 0.21 mmol) in acetone (20 mL) was diluted with hexane (200 mL) and divided in 70 mL portions. Each portion was degassed with Argon and was filled in a 100 mL ampoule (pyrex, ∅ = 3 cm). Each ampoule was placed in a water cooled pyrex photolysis vessel and irradiated with sixteen 300 nm lamps (25 W) in a Rayonet reactor for 45 min. The combined orange solutions were concentrated in vacuo to leave a red-brown amorphous solid. Polymeric impurities were removed by filtration over silica gel (20 g) with hexane/methyl-*tert*-butylether (5:1) as the eluent. Yield: 55 mg of **8** (69%), red-orange amorphous solid. M.p. 126–128 °C; ^{1}H NMR (300 MHz, CD_2Cl_2): $\delta = 1.75$ (dt, ^2J(28-H$_n$, 28-H$_x$) = 9.0 Hz, ^3J(28-H$_n$, 20-H) = ^3J(28-H$_n$, 27-H) = 1.6 Hz, 1H; 28-H$_n$), 2.14 (dt, ^3J(28-H$_x$, 20-H) = ^3J(28-H$_x$, 27-H) = 1.5 Hz, 1H; 28-H$_x$), 2.27 (dt, ^2J(17-H$_x$, 17-H$_n$) = 8.0 Hz, ^3J(17-H$_x$, 9-H) = ^3J(17-H$_x$, 16-H) = 1.5 Hz, 1H; 17-H$_x$), 2.64 (dt, ^3J(17-H$_n$, 9-H) = ^3J(17-H$_n$, 16-H) = 1.7 Hz, 1H; 17-H$_n$), 3.57 (m, 1H; 9-H), 3.63 (m, 1H; 16-H), 3.78 (m, 1H; 27-H), 4.38 (m, 1H; 20-H), 5.94 (s, 1H; 8-H), 6.20 (s, 1H; 3-H), 6.95–7.35 (m, 8H; 11-H, 12-H, 13-H, 14-H, 22-H, 23-H, 24-H, 25-H); ^{13}C NMR (75 MHz, CD_2Cl_2): $\delta = 49.31$ (C-28), 53.80 (C-16), 54.56 (C-27), 54.61 (C-20), 56.15 (C-9), 61.36 (C-17), 104.18 (C-5), 110.85 (C-4), 115.91 (C-19), 116.22 (C-18), 126.07 (C-8), 121.24, 121.81, 121.91, 122.18, 125.23, 125.23, 127.75, 127.97 (C-11, C-12, C-13, C-14, C-22, C-23, C-24, C-25), 142.48 (C-26), 145.03 (C-21), 147.62 (C-10), 148.23 (C-3), 148.31 (C-15), 148.97 (C-7), 150.94 (C-2), 158.76 (C-1), 171.03 (C-6); IR (KBr): $\tilde{\nu} = 2967$ (C–H), 2941 (C–H), 2861 (CH), 2210 (C≡N), 1636 (C=C), 757 cm^{-1} (C–H); MS (70 eV): m/z (%): 382 (100) [M^+], 355 (13) [$M^+ -$ HCN]; $C_{28}H_{18}N_2$: calcd 382.1470, found 382.1484 (MS).

Thermolysis of 20: A solution of **20** (2 mg, 4.4 μmol) and 1,1,2,2-tetrachloroethane (0.7 mg) as internal standard in CD_2Cl_2 (0.8 mL) was heated in a sealed NMR tube to 55 ± 1 °C. The time-dependent progress of the reaction was determined by ^{1}H NMR analysis of the signals at $\delta = 6.25$ and 6.04, assigned to **20** and 1,1,2,2-tetrachlorethane, respectively. The specific rate constant k_1 of the rearrangement **20** → **21** was calculated from the time-dependent decrease of **20** against the internal standard by the use of the kinetic law of irreversible first-order reactions (Table 9).

Table 9. Time dependence of reaction **20** → **21** in CD_2Cl_2 at 55 °C followed by ^{1}H NMR.[a]

t [s]	0	7200	14400	21600
20 [%]	100	61.7	30.4	26.8

[a] $k_1 = (6.5 \pm 1.1) \times 10^{-5}$ s^{-1}; $r = 0.972$.

X-Ray crystal structure determinations

Compound 4: $C_{16}H_{22}O$; crystal dimensions $0.43 \times 0.35 \times 0.01$ mm^3; measured on a Siemens P4-diffractometer with $Mo_{K\alpha}$ radiation; $T = 293$ K. Cell dimensions $a = 6.367(3)$, $b = 10.284(5)$, $c = 18.786(8)$ Å, $\beta = 96.81(4)°$, $V = 1221.3(1.0)$ Å^3; monoclinic crystal system; $Z = 4$; $\rho_{calcd} = 1.253$ g cm^{-3}; $\mu = 0.08$ mm^{-1}; space group $P2_1/c$; data collection: 2314 reflections of which 1521 were considered independent ($R_{merg} = 0.0649$, $2.18° \leq \Theta \leq 22.34°$) and 535 observed [$F_0 \geq 4\sigma(F)$]; structure solution with direct methods (SHELXS) and refinement on F (SHELXTL 4.2); parameters 155; hydrogen atom positions were calculated and refined as riding groups with common isotropic U values. $R = 0.0757$, $wR_w = 0.0572$, $w^{-1} = \sigma^2(F) + (0.0001 \times F^2)$; maximum residual electron density 0.24 e Å^{-3}.

Compound 6: $C_{24}H_{18}N_4$; crystal dimensions $0.19 \times 0.13 \times 0.05$ mm^3; measured on a Siemens SMART-CCD-diffractometer with $Mo_{K\alpha}$ radiation; $T = 298$ K. Cell dimensions $a = 9.3401(7)$, $b = 9.8337(8)$, $c = 11.1736(9)$ Å, $\alpha = 83.874(2)$, $\beta = 82.936(2)$, $\gamma = 73.270(2)°$, $V = 972.62(13)$ Å^3; triclinic crystal system; $Z = 2$; $\rho_{calcd} = 1.238$ g cm^{-3}; $\mu = 0.075$ mm^{-1}; space group $P\bar{1}$, data

Table 10. The cartesian coordinates for Becke3LYP/6-31G* optimized geometry of **6**.

atom label	atomic number	x	y	z
1	6	1.410504	1.381294	−1.996139
2	6	−1.345474	−0.666548	−0.243923
3	6	−3.100525	−0.451805	−1.738240
4	6	−3.425079	−1.935578	0.182889
5	6	−4.174087	−0.866540	−0.671786
6	6	−2.012298	−2.005765	−0.500509
7	6	−1.999664	0.269429	−0.976927
8	1	−3.099433	−2.588766	−2.348048
9	1	−3.357015	−1.668200	1.241796
10	1	−5.050135	−1.297533	−1.168150
11	6	−2.412072	−1.815698	−1.985680
12	6	−1.783955	1.696415	−0.772885
13	1	−1.550580	−1.746743	−2.656649
14	1	−3.504547	0.071989	−2.607820
15	1	−3.917430	−2.912123	0.123377
16	1	−4.517539	−0.011388	−0.081861
17	1	−1.436611	−2.899640	−0.250127
18	1	−2.526346	2.415674	−1.111872
19	6	−0.678225	2.077328	−0.109901
20	6	−0.259791	3.400539	0.488656
21	6	−0.354625	−0.246714	0.835911
22	6	0.357015	1.027158	0.329211
23	6	0.654807	−1.331990	1.171907
24	1	−0.916278	−0.013372	1.750919
25	6	1.207231	1.882888	1.343346
26	6	−0.656869	3.332279	1.996086
27	1	−0.635211	4.282626	−0.034681
28	6	1.275126	3.242101	0.602791
29	6	0.341272	2.273465	2.570576
30	1	1.793308	3.218263	−0.357858
31	1	2.163869	1.422674	1.602427
32	1	0.988965	2.715136	3.334763
33	1	−1.704508	3.050441	2.132682
34	1	−0.508976	4.310880	2.466320
35	1	−0.160459	1.424363	3.042635
36	1	1.732117	4.021592	1.221286
37	6	0.365560	−2.193786	2.267990
38	6	1.778454	−1.486948	0.414543
39	6	1.992619	−0.587160	−0.729897
40	6	2.728754	−2.522307	0.680915
41	6	1.267336	0.567408	−0.834288
42	6	2.939320	−0.970589	−1.731964
43	7	1.500488	2.051075	−2.944593
44	7	3.712340	−1.292943	−2.538758
45	7	3.507692	−3.357578	0.899117
46	7	0.067308	−2.859000	3.176343

collection 3374 relections, of which 2408 were considered independent ($R_{merg} = 0.0297$, $2.17^\circ \le \Theta \le 22.50^\circ$) and 1568 observed [$F_0 \ge 4\sigma(F)$]; absorption correction with Siemens SADABS programme: R_{merg} before/after: 0.0334/0.0277, max/min transmission: 1.00/0.47; structure solution with direct methods (SHELXS) and refinement on F^2 (SHELXTL 5.03); parameters 253; hydrogen atom positions were calculated and refined as riding groups with the 1.2-fold isotropic U values of the corresponding C atoms. $R1 = 0.0667$, $wR2$(all data) $= 0.2048$, $w^{-1} = \sigma^2(F_o^2) + (0.1257 \times P)^2$, where $P = [(\max F_o^2) + (2F_c^2)]/3$; maximum residual electron density 0.206 e Å^{-3}.

Compound 7: $C_{20}H_{18}N_2$; crystal dimensions $0.66 \times 0.35 \times 0.11$ mm^3; measured on a Siemens P4 diffractometer with $Mo_{K\alpha}$ radiation; $T = 298$ K. Cell dimensions $a = 10.453(1)$, $b = 14.593(1)$, $c = 10.4524(6)$ Å, $\beta = 91.142(6)^\circ$, $V = 1594.09(24)$ Å^3; monoclinic crystal system; $Z = 4$; $\rho_{calcd} = 1.193$ g cm^{-3}; $\mu = 0.07$ mm^{-1}; space group $P2_1/c$; data collection: 5251 reflections of which 2816 were considered independent ($R_{merg} = 0.0204$, $1.95^\circ \le \Theta \le 25.0^\circ$) and 2289 observed [$F_0 \ge 4\sigma(F)$]; structure solution with direct methods (SHELXS) and refinement on F^2 (SHELXTL 5.03); parameters 200; hydrogen atom positions were calculated and refined as riding groups with 1.2-fold isotropic U values of the corresponding C atoms. $R1 = 0.0701$, $wR2$(all data) $= 0.1799$, $w^{-1} = \sigma^2(F_o^2 + (0.1159 \times P)^2 + 0.1524 \times P$, where $P = [(\max F_o^2) + (2F_c^2)]/3$; maximum residual electron density 0.378 e Å^{-3}.

Compound 14: $C_{23}H_{17}N_3$; crystal dimensions $0.32 \times 0.28 \times 0.15$ mm^3; measured on a Siemens SMART-CCD-diffractometer with $Mo_{K\alpha}$ radiation; $T = 298$ K. Cell dimensions $a = 10.1026(2)$, $b = 11.3405(2)$, $c = 15.5570(3)$ Å, $\beta = 96.5200(10)^\circ$, $V = 1770.81(6)$ Å^3; monoclinic crystal system; $Z = 4$, $\rho_{calcd} = 1.258$ g cm^{-3}; $\mu = 0.075$ mm^{-1}; space group $P2_1/n$; data collection: 11 261 reflections of which 2743 were considered independent ($R_{merg} = 0.0427$, $2.23^\circ \le \Theta \le 24.10^\circ$) and 2206 observed [$F_0 \ge 4\sigma(F)$]; absorption correction with Siemens SADABS programme: R_{merg} before/after: 0.0845/0.0416, max/min transmission: 1.00/0.61; structure solution with direct methods (SHELXS) and refinement on F^2 (SHELXTL 5.03); parameters 236; hydrogen atom positions were calculated and refined as riding groups with 1.2-fold isotropic U values of the corresponding C atoms. $R1 = 0.0602$, $wR2$(all data) $= 0.1635$, $w^{-1} = \sigma^2(F_o^2) + (0.0825 \times P)^2 + 0.64 \times P$, where $P = [(\max F_o^2) + (2F_c^2)]/3$; maximum residual electron density 0.344 e Å^{-3}.

Cartesian coordinates for Becke3LYP/6-31G* optimized geometries of 6 and 22–26: The cartesian coordinates for Becke3LYP/6-31G* optimized geometries of **6** and **22–26** are given in Tables 10–15.

Table 11. The cartesian coordinates for Becke3LYP/6-31G* optimized geometry of **24**.

atom label	atomic number	x	y	z
1	1	−1.308731	−2.237659	1.393317
2	6	1.311984	0.052745	−0.072819
3	6	2.439670	1.063295	1.681760
4	6	3.182481	1.591223	−0.589283
5	6	2.927585	2.262937	0.796979
6	6	2.808996	0.088748	−0.325188
7	6	1.088021	0.638899	1.127022
8	1	4.404693	0.125680	1.225386
9	1	2.579306	2.028261	−1.391487
10	1	3.850043	2.691365	1.205946
11	6	3.330071	−0.073220	1.124198
12	6	−0.257174	0.983699	1.573601
13	1	3.093510	−1.051473	1.553512
14	1	2.483750	1.251727	2.758197
15	1	4.234597	1.677114	−0.885470
16	1	2.183692	3.064260	0.751609
17	1	3.192314	−0.609588	−1.072997
18	1	−0.400476	1.719768	2.363460
19	6	−1.294427	0.424045	0.927957
20	6	−2.769148	0.764084	0.944571
21	6	0.179609	−0.298351	−1.030889
22	6	−1.074225	−0.627002	−0.175713
23	6	0.542808	−1.444813	−1.957464
24	1	−0.021875	0.594556	−1.644735
25	6	−2.486100	−0.576442	−0.872686
26	6	−2.990811	1.739073	−0.251748
27	1	−3.153339	1.137311	1.897966
28	6	−3.415056	−0.518159	0.366582
29	6	−2.753730	0.818752	−1.494439
30	1	−3.342356	−1.391019	1.020284
31	1	−2.648763	−1.410382	−1.559420
32	1	−3.646520	0.774493	−2.128192
33	1	−2.308896	2.593526	−0.216189
34	1	−4.016756	2.126846	−0.235800
35	1	−1.936109	1.172130	−2.128878
36	1	−4.467825	−0.372617	0.098459
37	1	1.021009	−1.210342	−2.905781
38	6	0.338833	−2.716703	−1.579709
39	6	−0.265565	−2.998510	−0.277354
40	1	0.638948	−3.546564	−2.215538
41	6	−0.882400	−2.027710	0.416450
42	1	−0.198739	−4.006942	0.125386

Table 12. The cartesian coordinates for Becke3LYP/6-31G* optimized geometry of **25**.

atom label	atomic number	x	y	z
1	6	2.172348	0.268127	1.215195
2	6	1.005541	−0.213154	1.869349
3	1	1.059856	−0.641428	2.866836
4	6	−0.196419	−0.213758	1.151791
5	1	3.119182	0.337566	1.745614
6	6	2.070747	0.585814	−0.112385
7	1	2.923590	0.933057	−0.688526
8	6	0.754044	0.412310	−0.768722
9	6	−1.111005	−1.293536	−1.131564
10	1	0.755292	0.723410	−1.820985
11	6	0.915433	−2.351027	−0.658238
12	1	−1.089740	−0.600566	1.642744
13	6	0.152163	−1.035887	−0.555313
14	6	−0.401203	0.983831	0.108191
15	6	−0.415414	2.427149	0.662046
16	6	−2.438888	2.204034	−0.353760
17	6	−2.071506	−0.260108	−1.219998
18	6	−1.133149	−2.747349	−1.551416
19	6	−1.723289	0.895935	−0.572945
20	1	−3.036818	−0.401513	−1.701318
21	1	−0.154076	4.431693	−0.177545
22	1	0.319136	2.605392	1.449266
23	1	−2.221373	1.874168	1.835405
24	6	−1.719474	3.280048	−1.226425
25	6	−1.904252	2.574428	1.055027
26	1	−3.523580	2.171934	−0.488561
27	1	−2.273724	4.225806	−1.191243
28	1	−1.651181	2.975028	−2.275122
29	6	−0.322650	3.410115	−0.536026
30	1	0.506077	3.163471	−1.207036
31	1	−2.170992	3.593046	1.361135
32	1	−2.122674	−3.188526	−1.699534
33	6	−0.237384	−3.359904	−0.444047
34	1	−0.225508	−3.892866	−3.194367
35	1	1.782710	−2.435182	−0.000862
36	6	1.224990	−2.571744	−2.172643
37	1	−0.682329	−3.297898	0.554367
38	6	−0.180130	−2.876156	−2.785857
39	1	1.907747	−3.418959	−2.303344
40	1	1.704521	−1.696818	−2.623813
41	1	−0.454622	−2.184607	−3.588211
42	1	0.050952	−4.398308	−0.648392

0947-6539/99/0507-2130 $ 17.50+.50/0 *Chem. Eur. J.* **1999**, *5*, No. 7

Table 13. The cartesian coordinates for Becke3LYP/6-31G* optimized geometry of **26**.

atom label	atomic number	*x*	*y*	*z*
1	6	2.197989	0.266281	1.124868
2	6	1.064041	– 0.206712	1.794360
3	1	1.090609	– 0.469714	2.847718
4	6	– 0.149926	– 0.333413	1.032926
5	1	3.147847	0.386384	1.640310
6	6	2.062431	0.574894	– 0.219195
7	1	2.893550	0.947174	– 0.810744
8	6	0.747982	0.380976	– 0.824572
9	6	– 1.150332	– 1.293019	– 1.117809
10	1	0.695978	0.638726	– 1.887307
11	6	0.859747	– 2.374156	– 0.561916
12	1	– 1.016139	– 0.705348	1.586369
13	6	0.110558	– 1.037804	– 0.429468
14	6	– 0.426256	0.982462	0.087940
15	6	– 0.411994	2.407860	0.663937
16	6	– 2.446068	2.206766	– 0.330386
17	6	– 2.096568	– 0.278834	– 1.201578
18	6	– 1.133899	– 2.723217	– 1.596420
19	6	– 1.733280	0.896668	– 0.555960
20	1	– 3.059906	– 0.410490	– 1.689266
21	1	– 0.143873	4.417515	– 0.166976
22	1	0.335817	2.570147	1.442012
23	1	– 2.210494	1.868190	1.854264
24	6	– 1.728519	3.283013	– 1.206696
25	6	– 1.895406	2.569888	1.074552
26	1	– 3.532032	2.179408	– 0.454783
27	1	– 2.276307	4.232094	– 1.163225
28	1	– 1.672286	2.981785	– 2.257115
29	6	– 0.324071	3.399543	– 0.529576
30	1	0.496296	3.148641	– 1.209130
31	1	– 2.149475	3.590003	1.387383
32	1	– 2.112290	– 3.154346	– 1.825441
33	6	– 0.314243	– 3.376961	– 0.451653
34	1	– 0.136837	– 3.806644	– 3.225873
35	1	1.683907	– 2.499222	0.142411
36	6	1.258290	– 2.547501	– 2.054155
37	1	– 0.825630	– 3.344580	0.516324
38	6	– 0.106322	– 2.809623	– 2.770000
39	1	1.935572	– 3.400734	– 2.170662
40	1	1.778817	– 1.666695	– 2.442875
41	1	– 0.322605	– 2.080453	– 3.556662
42	1	– 0.021724	– 4.411887	– 0.667162

Table 14. The cartesian coordinates for Becke3LYP/6-31G* optimized geometry of **22**$^+$.

atom label	atomic number	*x*	*y*	*z*
1	6	2.179216	0.260492	1.242201
2	6	1.012240	– 0.229724	1.915354
3	6	1.098155	– 0.761239	3.231337
4	6	– 0.212082	– 0.228645	1.189047
5	6	3.425223	0.378723	1.937718
6	6	2.067670	0.585103	– 0.099988
7	6	3.151557	1.081136	– 0.868754
8	6	0.739439	0.394104	– 0.754091
9	6	– 1.103178	– 1.294451	– 1.139011
10	1	0.748362	0.730183	– 1.795117
11	6	0.926777	– 2.365565	– 0.671601
12	6	– 1.377665	– 0.739275	1.861142
13	6	0.174015	– 1.047757	– 0.577132
14	6	– 0.398237	0.972863	0.130420
15	6	– 0.410912	2.416209	0.685422
16	6	– 2.424182	2.198421	– 0.358824
17	6	– 2.056645	– 0.257132	– 1.237700
18	6	– 1.136402	– 2.744355	– 1.550504
19	6	– 1.717834	0.891042	– 0.571695
20	1	– 3.016827	– 0.395795	– 1.726291
21	1	– 0.131262	4.411465	– 0.150993
22	1	0.311215	2.593077	1.484344
23	1	– 2.245793	1.887588	1.838400
24	6	– 1.673853	3.259452	– 1.231414
25	6	– 1.905264	2.571765	1.055680
26	1	– 3.504826	2.172026	– 0.513301
27	1	– 2.229383	4.203095	– 1.211571
28	1	– 1.588809	2.948132	– 2.276651
29	6	– 0.291337	3.392384	– 0.516212
30	1	0.551882	3.152964	– 1.171309
31	1	– 2.165379	3.596040	1.342124
32	1	– 2.129952	– 3.173492	– 1.694547
33	6	– 0.235886	– 3.361682	– 0.447631
34	1	– 0.254166	– 3.879986	– 3.202412
35	1	1.796619	– 2.457704	– 0.019136
36	6	1.225831	– 2.585842	– 2.190106
37	1	– 0.675053	– 3.304018	0.552523
38	6	– 0.186795	– 2.866561	– 2.793183
39	1	1.892782	– 3.444580	– 2.315627
40	1	1.721490	– 1.723356	– 2.646912
41	1	– 0.458396	– 2.169744	– 3.591497
42	1	0.041671	– 4.399308	– 0.660829
43	7	– 2.343626	– 1.159393	2.354329
44	7	1.164800	– 1.196919	4.310027
45	7	4.437719	0.479635	.499748
46	7	4.002247	1.491630	– 1.552711

Acknowledgements

We are grateful to the Deutsche Forschungsgemeinschaft, Ministerium für Wissenschaft und Forschung des Landes Nordrhein-Westfalen, Fonds der Chemischen Industrie, and to the National Science Foundation for financial support, and the National Center for Supercomputing Applications (NCSA) and UCLA Office of Academic Computing for computer time.

[1] O. Ermer, F.-G. Klärner, M. Wette, *J. Am. Chem. Soc.* **1986**, *108*, 4908 – 4911.
[2] Review: G. I. Fray, R. G. Saxton, *The Chemistry of Cyclooctatetraene and its Derivatives*, Cambridge University Press, **1978**.
[3] P. G. Wenthold, D. A. Hrovat, W. T. Borden, W. C. Lineberger, *Science* **1996**, *272*, 1456 – 1459.
[4] F. W. B. Einstein, A. C. Willis, W. R. Cullen, R. L. Soulen, *J. Chem. Soc. Chem. Commun.* **1981**, 526 – 528; H. Dürr, G. Klauck, K. Peters, H. G. von Schnering, *Angew. Chem.* **1983**, *95*, 321; *Angew. Chem. Int. Ed. Engl.* **1983**, *22*, 332 – 333; *Angew. Chem. Suppl.* **1983**, 347 – 362.
[5] M. A. P. Bowe, R. G. J. Miller, J. B. Rose, D. G. M. Wood, *J. Chem. Soc.* **1960**, 1541 – 1547; T. Toda, T. Ohya, T. Mukai, *Bull. Chem. Soc. Jpn.* **1972**, *45*, 1561 – 1562.
[6] It is interesting to note that the corresponding Diels – Alder reaction between 5,6-bismethylene-2-norbornene and norbornadiene proceeds nonstereoselectively: J. Benkhoff, R. Boese, F.-G. Klärner, *Liebigs Ann./Recueil* **1997**, 501 – 516.
[7] K. B. Wiberg, M. G. Matturro, P. J. Okarma, M. E. Jason, *J. Am. Chem. Soc.* **1984**, *106*, 2194 – 2200; L. A. Paquette, H. Künzer, K. E. Green, *J. Am. Chem. Soc.* **1985**, *107*, 4788 – 4790; P. D. Bartlett, R. Banavali, *J. Org. Chem*. **1991**, *56*, 6043 – 6050.
[8] K. Saito, T. Mukai, *Bull. Chem. Soc. Jpn.* **1975**, *48*, 2334 – 2335.
[9] J. J. P. Stewart, *J. Comput. Chem.* **1989**, *10*, 209 – 214, 221 – 232.
[10] J. Bordner, R. G. Parker, R. H. Stanford, *Acta Crystallogr. Sect. B* **1972**, *28*, 1069 – 1075.
[11] L. A. Paquette, M. J. Carmody, *J. Am. Chem. Soc.* **1975**, *97*, 5841 – 5850; Review: R. W. Alder, W. Grimme, *Tetrahedron* **1981**, *37*, 1809 – 1812.
[12] G. Maier, N. H. Wiegand, S. Baum, R. Wüllner, W. Mayer, R. Boese, *Chem. Ber.* **1989**, *122*, 767 – 779.
[13] M. Ōki, *Applications of Dynamic NMR Spectroscopy to Organic Chemistry,* VCH, Deerfield Beach, **1985**, and references therein.

Table 15. The cartesian coordinates for Becke3LYP/6-31G* optimized geometry of **23**$^+$.

atom label	atomic number	*x*	*y*	*z*
1	6	2.938551	0.000000	– 0.016008
2	6	2.313286	0.000000	1.251817
3	6	3.061204	0.000000	2.455111
4	6	0.845163	0.000000	1.261919
5	6	4.366709	0.000000	– 0.132205
6	6	2.118528	0.000000	– 1.149469
7	6	2.618232	0.000000	– 2.474579
8	6	0.662327	0.000000	– 0.914187
9	6	– 1.225041	– 1.165473	0.281766
10	1	0.078761	0.000000	– 1.836552
11	6	0.681156	– 2.550524	0.166295
12	6	0.249459	0.000000	2.591020
13	6	0.238597	– 1.078997	0.169213
14	6	0.238597	1.078997	0.169213
15	6	0.681156	2.550524	0.166295
16	6	– 1.588025	2.618569	0.361225
17	6	– 1.980112	0.000000	0.303715
18	6	– 1.588025	– 2.618569	0.361225
19	6	– 1.225041	1.165473	0.281766
20	1	– 3.062510	0.000000	0.393923
21	1	0.657212	4.168974	– 1.299718
22	1	1.73350	2.706222	0.408687
23	1	– 0.286601	2.779269	2.160896
24	6	– 1.323742	3.224195	– 1.060363
25	6	– 0.356897	3.162606	1.138507
26	1	– 2.580872	2.830509	0.763215
27	1	– 1.694990	4.254117	– 1.086253
28	1	– 1.839982	2.668487	– 1.848727
29	6	0.231642	3.167122	– 1.187369
30	1	0.566695	2.579284	– 2.047436
31	1	– 0.325740	4.256929	1.164630
32	1	– 2.580872	– 2.830509	0.763215
33	6	– 0.356897	– 3.162606	1.138507
34	1	– 1.694990	– 4.254117	– 1.086253
35	1	1.733507	– 2.706222	0.408687
36	6	0.231642	– 3.167122	– 1.187369
37	1	– 0.286601	– 2.779269	2.160896
38	6	– 1.323742	– 3.224195	– 1.060363
39	1	0.657212	– 4.168974	– 1.299718
40	1	0.566695	– 2.579284	– 2.047436
41	1	– 1.839982	– 2.668487	– 1.848727
42	1	– 0.325740	– 4.256929	1.164630
43	7	– 0.272939	0.000000	3.628271
44	7	3.669412	0.000000	3.450316
45	7	5.524397	0.000000	– 0.234545
46	7	2.969226	0.000000	– 3.587400

[14] J. E. Leffler, E. Grunwald, *Rates and Equilibria of Organic Reactions*, Wiley, New York, **1963**; L. P. Hammet *Physical Organic Chemistry*, 2nd edition, McGraw-Hill, New York, **1970**; H. M. J. Boots, P. K. DeBokx, *J. Phys. Chem.* **1989**, *93*, 8240 – 8243; Z. Slanina, *Z. Phys. Chem. (Leipzig)* **1989**, *270*, 81 – 88.

[15] The spectral properties are consistent with those of 1,2,3-tricyanoazulene: S. Kuroda, M. Funamizu, Y. Kitahara, *Tetrahedron Lett.* **1975**, 1973 – 1974.

[16] O. W. Webster, *J. Org. Chem*. **1967**, *32*, 39 – 42.

[17] S. M. Hubig, J. K. Kochi, *J. Phys. Chem.* **1995**, *99*, 17578 – 17585.

[18] R. A. Marcus, *J. Phys. Chem*. **1989**, *93*, 3078 – 3086.

[19] C. D. Weis, *J. Org. Chem.* **1963**, *28*, 74 – 78.

[20] C. K. Bradsher, D. A. Hunt, *J. Org. Chem.* **1981**, *46*, 4608 – 4610.

[21] U. W. Naatz, Dissertation, Universität GH Essen, **1999**.

[22] A formal [1,5] vinyl shift is also observed in the thermolysis of spiro-[4.4]nonatetraene by M. F. Semmelhack, H. N. Weller, J. S. Foos, *J. Am. Chem. Soc*. **1977**, *99*, 292 – 294; M. F. Semmelhack, H. N. Weller, J. Clardy, *J. Org. Chem.* **1978**, *43*, 3791 – 3792.

[23] K. N. Houk, B. R. Beno, M. Nendel, K. Black, H. Y. Yoo, S. L. Wilsey, J. K. Lee, *J. Mol. Struct. (Theochem)* **1997**, *398 – 399*, 169.

[24] E. Goldstein, B. R. Beno, K. N. Houk, *J. Am. Chem. Soc.* **1996**, *118*, 6036 – 6043, and references therein; B. R. Beno, S. L. Wilsey, K. N. Houk, *J. Am. Chem. Soc*, in press; J. Tian, K. N. Houk, F.-G. Klärner, *J. Phys. Chem. A.* **1998**, *102*, 7662 – 7667.

[25] K. N. Houk, M. Nendel, O. Wiest, J. W. Storer, *J. Am. Chem. Soc.* **1997**, *119*, 10545 – 10548; B. R. Beno, S. L. Wilsey, K. N. Houk, unpublished results.

[26] B. R. Beno, K. N. Houk, D. A. Singleton, *J. Am. Chem. Soc.* **1996**, *118*, 9984 – 9985.

[27] M. J. Frisch, G. W. Trucks, H. B. Schlegel, P. M. W. Gill, B. G. Johnson, M. A. Robb, J. R. Cheeseman, T. A. Keith, G. A. Petersson, J. A. Montgomery, K. Raghavachari, M. A. Al-Latham, V. G. Zakrzewski, J. V. Ortiz, J. B. Foresman, J. Cioslowski, B. B. Stefanov, A. Nanayakkara, M. Challacombe, C. Y. Peng, P. Y. Ayala, W. Chen, M. W. Wong, J. L. Andres, E. S. Replogle, R. Gomperts, R. L. Martin, D. J. Fox, J. S. Binkley, D. J. Defrees, J. Baker, J. J. P. Stewart, M. Head-Gordon, C. Gonzalez, J. A. Pople, *Gaussian 94 (Revision C.2)*, Gaussian, Pittsburgh, PA, **1995**.

[28] A. D. Becke, *J. Chem. Phys.* **1993**, *98*, 5648 – 5652; C. Lee, W. Yang, R. G. Parr, *Phys. Rev. B* **1988**, *37*, 785 – 789.

[29] B. R. Beno, J. Fennen, K. N. Houk, H. J. Lindner, K. Hafner, *J. Am. Chem. Soc.* **1998**, *120*, 10490 – 10493.

Received: December 1, 1998 [F1468]